Applied Surface Science Advances 26 (2025) 100707

Contents lists available at ScienceDirect

Applied Surface Science Advances

journal homepage: www.sciencedirect.com/journal/applied-surface-science-advances

Review Article

Plasma Electrolytic Oxidation (PEO) coatings on aluminum alloy 2024: A review of mechanisms, processes, and corrosion resistance enhancement

Matteo Gamba [a,*], Andrea Cristoforetti [b], Michele Fedel [b], Federica Ceriani [a], Marco Ormellese [a], Andrea Brenna [a]

[a] Department of Chemistry, Materials and Chemical Engineering "Giulio Natta", Politecnico di Milano, Via Mancinelli 7, 20131 Milan, Italy
[b] Department of Industrial Engineering, University of Trento, 38123 Trento, TN, Italy

ARTICLE INFO

Keywords:
Plasma Electrolytic Oxidation
Aluminum
AA2024
Anodizing
Coating
Corrosion

ABSTRACT

AA2024, containing around 4% Cu and 1.5% Mg, has outstanding mechanical properties among the aluminum alloys, but poor corrosion resistance. Because of its substantial tensile strength, fatigue and wear resistance, it finds broad application in the aeronautical field. Its use, however, requires the application of a coating for ensuring adequate durability to the components. Plasma Electrolytic Oxidation (PEO) is a plasma-based coating process which has been object of growing interest in recent years because of its ability at producing thick and protective coatings by using simple, water-based electrolytes, thus reducing the environmental and safety risks presented by traditional anodizing processes. This is a promising technique for AA2024 coating, although it involves many different parameters, often interacting with each other. Thus, when optimizing it for this specific material, different effects should be considered, among which the main ones are the electrical input applied to the workpiece, the composition of the electrolytic solution and the presence of pre- or post-treatment.

In the present review the main features of the PEO coating of AA2024 are treated. The main process parameters are discussed and a complete description of the discharge mechanism and of the coating growth is given. Then, the properties of the PEO coatings grown upon AA2024 are treated, mainly from the point of view of corrosion resistance enhancement. Finally, some insights into the upscaling of PEO for its industrial application are given.

1. Introduction

Plasma discharge phenomena in aqueous electrolytes have been known since the late 19th century, even though only in the recent decades they have been exploited for producing ceramic layers upon metals. The first attempts with aluminum date back to the 1970s, then further progress has been made, and in recent years some companies have started applying plasma oxidation to the commercial scale [1–4].

Aluminum alloy 2024 is one of the most used alloys in the fields of aeronautical and aerospace applications, mainly because of its excellent mechanical properties [4]. Indeed, its microstructure characterized by the presence of micro-sized intermetallic precipitates offers high specific strength and modulus without reducing toughness, even at low temperatures [4]. Furthermore, its low density allows for fuel saving and its low melting temperature ensures optimal workability with different techniques (casting, plastic deformation, machining, welding) [4]. However, aluminum 2024 is one of the worst choices for corrosion resistance [4,5]. The intermetallic precipitates promote localized corrosion forms such as pitting or intergranular corrosion, and also abrasion and erosion strength are quite low [5]. Thus, a hard dielectric coating such as the one produced by Plasma Electrolytic Oxidation (PEO) is required for its use [5].

In addition to corrosion resistance, a PEO coating can give to the aluminum substrate properties which are usually typical of heavier materials, thus making it a suitable material choice also for demanding applications [1]. PEO-coated AA2024 features high surface hardness, high resistance to thermal shocks and thermal cycles, high adherence to the substrate [1] and good thermal [3] and electrical [6] insulation.

Nowadays, the practice of producing ceramic coatings upon metals by means of plasma discharges is addressed with various names. PEO is the most used one, but also Anodic Spark Deposition (ASD), Micro-arc Oxidation (MAO), and Plasma Chemical Oxidation (PCO) are used [1,

* Corresponding author.
E-mail addresses: matteo.gamba@polimi.it (M. Gamba), andrea.cristoforetti@unitn.it (A. Cristoforetti), michele.fedel@unitn.it (M. Fedel), federica.ceriani@polimi.it (F. Ceriani), marco.ormellese@polimi.it (M. Ormellese), andrea.brenna@polimi.it (A. Brenna).

https://doi.org/10.1016/j.apsadv.2025.100707
Received 17 December 2024; Received in revised form 22 January 2025; Accepted 24 January 2025

2]. The reasons why these coatings are gaining growing attention are their thickness, ranging from tenths to hundreds of micrometers [2], and their properties, such as high thickness, hardness, density, and adherence [1–4]. Furthermore, the PEO process is usually simpler, less hazardous, and more environmentally friendly than other coating processes [2,7,8], it has no risks of shape distortion or substrate modification [4,8] and it is cost-saving if compared to other techniques [8,9].

This review deals with the PEO coating of aluminum alloy 2024: on this application of plasma anodizing the interest has been growing recently, thus a quite complete overview is available by comparing different literature studies, even though some aspects still require clarification. The knowledge on the PEO mechanism and on the structure of the resulting coatings, object of the following sections, is quite full and exhaustive. Concerning the electrolyte composition optimization, instead, a lot of work has been carried out recently, taking into account a large number of additives which can be used for modifying the PEO layers. Despite this, since most of the works have been carried out with an empirical approach, a complete understanding of the additives action has not been reached for all of them. Concerning the electrical parameters controlling the plasma and the discharge features, deeper explanations are available. Finally, a section is reserved to the challenges PEO has to face for approaching large-scale applications, where further investigation is still required.

2. Plasma anodizing processes

A PEO coating has a complex architecture resulting in a high wear and corrosion resistance [2,3]. As shown by Fig. 1, it is characterized by an inner, nanometric defect-free barrier layer, a rather compact intermediate layer, and a porous outer layer, whose thicknesses are dependent on the process parameters [1,2,9]. Among them, the inner ones seem to provide the highest contribution to corrosion protection [9].

This oxide layer is generated, similarly to traditional anodic oxidation of metals, by the reaction between the anode metal and the oxygen dissolved into the electrolyte forming a passive, insoluble layer upon its surface. It is common knowledge that this can occur only with the so-called “valve-metals”, endowed with an oxide exhibiting a low electron conductivity and a higher ionic conductivity [1,3]. This layer has a significant electric resistance, thus slowing down the corrosion process [1,3]. For PEO processes, then, it is required to allow plasma ignition so that the metal shows a passive behavior into the chosen electrolyte over a sufficiently wide range of potential [1,3]. Most aluminum alloys, among which the whole AA2xxx series, meet these requirements thanks to the high bandgap of alumina [3].

3. PEO mechanism

The main phases of the PEO process are represented in Fig. 2a. The thin oxide layer formed on the anode surface because of passivation into an alkaline electrolyte is essential for the process activation [1,3,4,10]. Indeed, due to the increased resistivity at the anode/electrolyte interface, a potential increase is required to make current flow into the cell. If the potential applied rises enough, the electric field in the aforementioned region reaches the critical value at which dielectric breakdown occurs, and a plasma discharge is activated. The voltage at which this occurs is named breakdown potential [1,2,9]. The channel thus activated rapidly grows until crossing the whole oxide thickness, and the temperature into it reaches some thousands of Kelvin degrees (8000K – 10000K). Metallic ions are thermally ejected from the substrate, reacting with the oxygen dissolved into the electrolyte and forming new oxide [1,2,9].

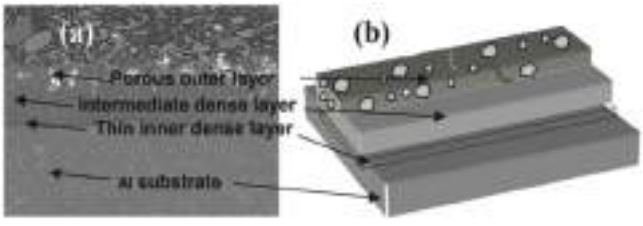

Fig. 1. (a) A SEM micrograph and (b) a schematic of a PEO coating obtained on an aluminum alloy. Adapted from [9].

In absence of discharges, the main reactions on the anode surface would be the formation of aluminate ions and the transformation of alumina into aluminum hydroxide (Eqs. (1) and (2)) [11].

$$2Al + 2H_2O + 2OH^- \rightarrow 2AlO_2^- + 3H_2 \quad (1)$$

$$Al_2O_3 + 2OH^- + 3H_2O \rightarrow 2Al(OH)_4^- \rightarrow 2Al(OH)_3 + 2OH^- \quad (2)$$

During the anodic plasma discharges, instead, the reactions occurring at the anode surface and leading to the coating formation are the metal dissolution and the metal oxide precipitation [2], given in Eqs. (3) and (4).

$$Al \rightarrow Al^{3+} + 3e^- \quad (3)$$

$$2\ Al^{3+} + 9\ H_2O \rightarrow Al_2O_3 + 6\ H_3O^+ \quad (4)$$

These reactions do not always follow the Faraday law, differently from conventional anodizing [2]. Indeed, the coating growth proceeds not by means of a continuous charge transport through the electrolyte and the oxide, but by means of a fast reaction between oxygen and aluminum ions occurring as the plasma sparks cool down [3].

The oxide growth proceeds both inward and outward, as in Fig. 2b [2] and increases locally the electric resistance, stopping the occurring discharge [1]. New discharges trigger where the electric field is higher or where the passive layer is thinner [1]. Every time a discharge begins, the underlying oxide locally re-melts and, after the end of the discharge, solidifies again. This promotes the formation of α-alumina, highly desirable for corrosion protection and surface hardness [1–3].

Plasma processes involve a large thermal and acoustic emission [2]. The localized heating of the surface decreases the breakdown voltage, thus increasing both the average discharge life and the probability of having new discharges where an old one occurred [1]. This mechanism could lead to the appearance of large, destructive sparks, but this depends on the chosen process parameters, and this event can be avoided or delayed for a very long time [1]. Discharge mechanisms will be addressed more in detail in paragraph 9.

The coating growth process here briefly depicted appears to be very complex, such that it still needs to be understood completely [9]. In the following, the main variables of these microarc processes will be addressed with a peculiar regard for results obtained over AA2024. In particular, the effects of the alloying elements, the electrolyte composition, the electrical input, and of the pre- and post-treatments will be treated. Then, some details about the properties of PEO-coated AA2024 will be given, with a special focus on its corrosion resistance and its tribological properties.

4. Effect of the alloying elements

The nature of the substrate has a strong influence on the PEO oxide layer [1,12]. During the process, not only the substrate metal but also its alloying elements, the precipitates and the reinforcements dispersed in the metallic matrix take part in the electrochemical reactions [1]. Not all of them, however, end up in the coating, since traces of the solute elements have been found also in the electrolyte [3]. The ones entering the coating can form mixed oxides or inclusions [3].

Alloy AA2024 is an Al-Cu-Mg alloy, containing 4.3%-4.5% Cu, 1.3%-1.5% Mg and 0.5%-0.6% Mn. Cu and Mg have been reported among the deleterious alloying elements for PEO [3] since, likewise to Zn, they obstacle the conversion of γ-alumina into the more stable α-alumina [1,8,12]. Comparison between alloys AA2024, AA6082 (Al-Si-Mg) and

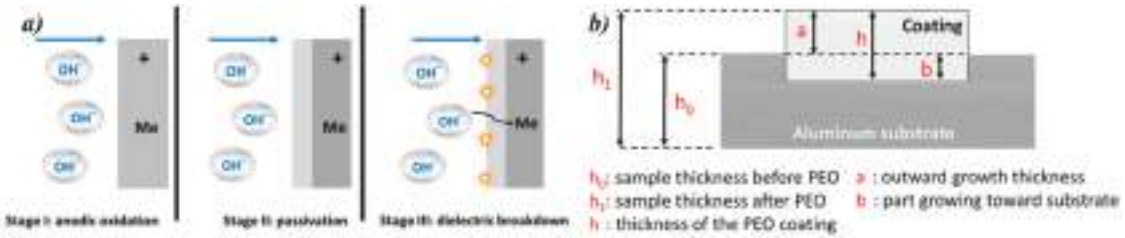

Fig. 2. Schematic diagram a) of the PEO reaction mechanism and b) of the growth of a PEO coating on an Al substrate. Adapted from [2].

AA7075 (Al-Zn-Mg) shows on the latter the lowest amount of α-alumina [13].

Magnesium seems to be the most effective element in increasing the γ-to-α phase transition temperature [12,13]. Copper instead forms dark inclusions of copper oxides and hydroxides into the inner part of the coating, which rearranges into a single dark layer as coating thickness increases (Fig. 3) [7,13,14]. There is also an effect of the alloying elements on the coating thickness, leading, after the same PEO process, to a thicker oxide on Al-Zn-Mg alloys (such as 7050 or 7075) than on Al-Cu-Mg (such as AA2024 or AA2214) or on Al-Si-Mg ones (AA6082) [13,15]. In general, it seems that the best results with PEO on Al alloys have been obtained with the least alloyed ones, such as AA1050 (Fig. 3b) [12]. However, not all the works agree on this point: Sieber et al., for example, reported some difficulties in PEO coating commercially pure aluminum [13]. The same electrolyte used for coating AA2024, AA6082 and AA7075 resulted to be too aggressive for the oxide formed on pure aluminum, thus requiring a reduction of the alkali content [13].

5. Effect of the electrolyte composition

The electrolyte composition plays a major role in the determination of the properties of the PEO coating [1–3]. Electrolyte constituents might take part in the plasma reactions or not, thus determining whether they will be incorporated into the coating [1,3]. Furthermore, the electrolyte might contain dissolved or dispersed additives, such as microparticles, which might enter the coating too [1,3].

Generally, solutions for Al PEO are alkaline [1], with a pH around 13 [3], even though the reasons for which such a high pH is required for PEO have not been fully clarified yet. The pH of the electrolyte is raised usually by adding NaOH or KOH. The higher the pH, the lower the growth rate, due to the enhanced anodic dissolution [16]. However, with higher amounts of NaOH, the roughness of the coating is lower, and the incorporation of electrolyte elements is higher [16]. Doolabi et al. have suggested 10 g/L as the maximum concentration of NaOH in the electrolyte since coatings produced in more alkaline solutions show a damaged inner coating layer which cannot offer proper protection from corrosion [16].

Conductivity between 5 and 100 mS cm^{-1} is required to reduce the voltage drop in the electrolyte, leaving more to create the field across the oxide, causing the dielectric breakdown [3]. This is particularly relevant since breakdown occurs at the bottom of the coating pores, which, being narrow and tall, provide a large ohmic drop [3]. Finally, electrolyte aging is an important parameter too, since during PEO it might get polluted or some of its elements might be depleted [2,3,17]. A common practice for facing electrolyte depletion in industrial processes is "correcting" it with the addition of the constituents consumed. However, this leads to a build-up of impurities, whose effect is addressed in paragraph 5.1 [17].

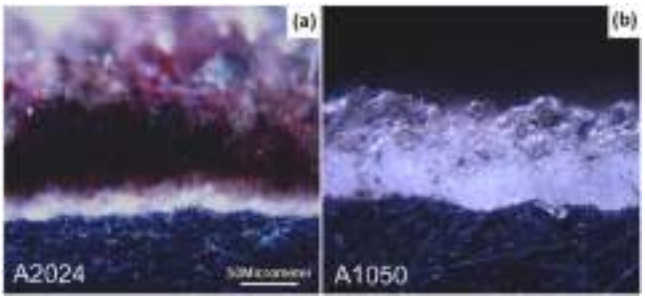

Fig. 3. Micrograph of a section of a PEO coating on a) AA2024 and b) AA1050, showing the formation of a dark, copper oxide-rich layer, in alloy 2024. Adapted from [7].

A lot of works available in literature on the PEO topic are related to the optimization of the electrolytic solution composition. Different methods of doing this have been explored in recent years, seldom with the support of algorithms for the design of experiments, such as the response surface methodology (RSM) [18], even though not yet with AA2024.

5.1. *Effect of the dissolved additives*

In this paragraph only dissolved additives are going to be considered, while dispersed particles electrolyte constituents are treated in the following.

5.1.1. *Sodium silicate (Na_2SiO_3)*

Sodium silicate (Na_2SiO_3) is one of the most used additives, not only with alloy AA2024 but also with Mg and Ti alloys. Its main effect is reducing the breakdown voltage value, helping the onset of plasma discharges at lower voltages [2,3,6]. Thus, PEO coatings grow faster and thicker in silicate-based electrolytes [2,14], even though with a quite large thickness fluctuation connected to the appearance on the surface of nodular protrusions [2]. In addition to this, the lower sparking voltage creates a colder plasma which is less able to convert γ-alumina into α-alumina: thus, coatings produced in the presence of silicates contain a lower fraction of α-alumina [6]. However, it must be considered also that the γ-to-α transition of alumina requires a coating able to keep the heat inside the oxide, and that this thermal insulation effect is less pronounced in thin coatings, which thus will show a lower fraction of α-alumina [14]. Lv et al. suggest that the silicon atoms coming from the electrolyte form mullite, a mixed oxide, with aluminum and oxygen ($3Al_2O_3{\bullet}2SiO_2$) [6], while other reported the formation of silicon oxide (SiO_2) [19]. These silicate-containing phases reduce the coating's hardness, increase its toughness, and make it more resistant to thermal shock [16]. The large inclusion of Si into the outer coating layer is driven by the strong electric field, attracting silicate anions (SiO_3^{2-}) inside the coating pores [6,19]. There, they react with protons forming a gel of hydrated silica, as in Eqs. (3) and (4), which would then block any further inward migration of electrolyte components [6].

$$SiO_3^{2-} + 2H^+ \rightarrow SiO_2 + H_2O \quad (3a)$$

$$SiO_2 + nH_2O \rightarrow SiO_2{\cdot}nH_2O \quad (4a)$$

If the area covered with the silica gel is then interested in a plasma discharge, silica and the underlying alumina might melt and solidify as mullite [6].

Different Na_2SiO_3 concentrations are used in literature for AA2024,

ranging from a few to some tenths of grams per liter. The only optimum study on this point has been performed by Liang et al. for Al 6064 [20]. According to them, coatings produced in quite diluted silicate solutions (around 10 g/L) show the best corrosion resistance, while at higher concentrations, porous and amorphous silica formation is favored rather than protective alumina and mullite [20].

5.1.2. Phosphate ions (PO_4^{3-})

Some attempts to use phosphate ions to reduce the breakdown potential of alloy 2024 have been made, even though with poorer results than with silicates [6,21]. On pure Al substrates, in an alkaline-phosphate electrolyte plasma discharges trigger at 300 V, while with silicates sparking occurs at 240 V and in a mixed electrolyte at 280 V [2]. Thus, the coating growth is slower with phosphates, even though the resulting coatings are often reported to be more homogeneous [2]. Due to the higher breakdown potential, phosphate plasma will be hotter than silicate one, thus the resulting coatings will contain a larger amount of α-alumina [6].

Phosphorous, differently from Si, is less active in the plasma, and is detected in a lower amount in the coating [2], homogeneously distributed throughout the whole thickness [6,21]. Lv et al. have proposed a justification for the homogeneous distribution of P in the coating thickness: since it is present in the electrolyte as HPO_4^{2-} or $H_2PO_4^-$, whose complete reduction is difficult, these groups do not deposit on the surface of the coating but are transported by the strong electric field into the pores, where they are involved into the discharges: thus, P results distributed in the whole coating thickness [6].

Fattah-Alhosseini et al. reported that the positive effect of $Na_2HPO_4 \bullet 2H_2O$ on the PEO coating of AA2024 in a phosphate-silicate electrolyte is highest at a concentration of 10 g/L, obtaining an average pore size of 1.43 μm, increasing at higher concentrations, as depicted in Fig. 4 [21]. This is reflected in an enhanced corrosion resistance [21].

5.1.3. Glycerin ($C_3H_8O_3$)

Hossein et al. introduced glycerin during the PEO of alloy AA2024 to increase the viscosity of the electrolyte [5,22]. Indeed, as the dissipated heat grows, the temperature of the electrolyte close to the specimen surface increases up to the boiling point, and the process becomes very turbulent with a lot of splashing out. Glycerin addition is successful in limiting the electrolyte turbulence near the surface, thus improving the coating homogeneity [5,22]. The ceramic layer produced in the presence of glycerin is less porous and less cracked, thus more resistant to corrosion [5], and offers an enhanced wear resistance too [22].

5.1.4. Effect of dissolved cations

Being that the valve metal oxides, such as alumina, show a low electronic conductivity and a non-negligible cationic conductivity, the cationic composition of the electrolyte becomes an important factor during PEO [23]. In AA2024 PEO electrolytes, Na^+ and K^+ are the most common cations in concentrations between 10^{-1} M and 10^{-3} M, while there is a lack of information about the use of other cations [23]. Indeed, the main electrolyte ingredients are NaOH, KOH, Na_2SiO_3 or Na_2HPO_4.

The positive ion behavior in an aqueous solution mainly depends on its ionic radius and its charge density, respectively controlling the number of water molecules in its first coordination sphere and the strength of its bond to them [23]. These control the cation mobility and, thus the electrical conduction in the electrolyte: for instance, the valve effect is more pronounced if Na^+ or K^+ are found in the electrolyte, while it is less intense with Ca^{2+} [23,24].

By PEO coating commercially pure aluminum in different electrolytes, Rogov and Shayapov [23] reported that in the absence of singly charged cations, crystalline alumina does not form. K and Na are included in the coating only in very small amounts, while Ca appears in the coating in a higher amount [23]. Furthermore, different cations such as Na^+ and K^+, despite having the same charge, produce different coating microstructures, as shown in Fig. 5.

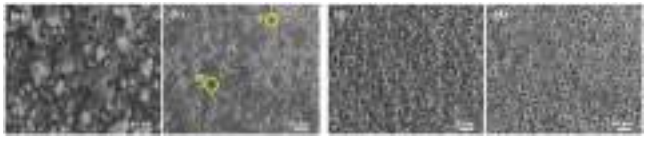

Fig. 4. Surface morphology of PEO coated AA2024 specimens at different concentrations of Na2HPO4•2H2O: a) 5 g/L, b) 10 g/L, c) 15 g/L, d) 20 g/L. Adapted from [21].

5.1.5. Hydrogen peroxide

An attempt to use hydrogen peroxide (H_2O_2) as an additive during the PEO of AA2024 has been made by Posuvailo et al. to accelerate the growth process. The decomposition of hydrogen peroxide, indeed, is supposed to provide an extra amount of oxygen in the reaction sites [25]. An H_2O_2 concentration of 5 g/L has been individuated as the optimum for pore size decrease and thickness increase. This has been confirmed also by Student et al. [26]. Furthermore, the presence of hydrogen peroxide increases also the α-alumina over γ-alumina ratio [25]. A drawback in the use of hydrogen peroxide is its fast exhaustion, motivated by the velocity of its degradation: for this reason, some proposals for replacing it with oxygen or ozone bubbling have been advanced, even though with porosity increase [27]. However, no information is available about the effect of hydrogen peroxide on the coating's corrosion resistance.

5.1.6. Organic compounds

There are some notices of the use of organic compounds other than glycerin in the PEO of Al-Cu-Mg alloys. For instance, potassium tartrate ($C_4H_4O_6K_2 \bullet 0.5H_2O$) has been used by Egorkin et al. during the PEO of Al D16T alloy, analogous to AA2024, as a source of carbon. The aim was to form carbide inclusions for hardness improvement, introducing also salts of carbide-forming metals such as W, Co, and Mo [28].

Organic chelating agents, such as EDTA-2Na, have been proposed for softening the plasma discharges, thus inhibiting the onset of potentially destructive sparks [29]. In their presence, the discharges become softer and more homogeneous, until anticipating an eventual transition to soft sparking [29,30]. Zhang et al. reported that with the addition of EDTA-2Na, the amount of electrolyte elements in the coating increases and the outer porous layer becomes thinner and more compact, resulting in an improved corrosion resistance [29]. The reason for this can be found in its ability to coordinate cations, forming negatively charged complexes which thus are attracted toward the anodically-polarized substrate [30].

More complex organic molecules such as acrylic acid or polyacrylic acid have been tested on other Al alloys, such as AA6061. These molecules are embedded in the coating, providing an enhancement of the anticorrosion behavior, even though their incorporation is difficult since organic molecules are prone to be destroyed by plasma discharges [31]. Finally, some organic acids such as acetic, lactic or citric might be used as plasma softening additives in PEO. However, there are examples of their use only with Ti-based alloys [19,32].

5.1.7. Other additives

There is then a large set of other additives for AA2024 PEO whose use is seldom reported in the literature. Tungsten salts (Na_2WO_4) have proved to produce the incorporation of tungsten oxide (WO_3) into the coating [10,33], which in turn shows higher adhesion, lower porosity, and a darker color [10].

Sodium aluminate ($NaAlO_2$) has been tested during the PEO of alloy AA2024 [34–36], but there are examples also with Al-Si cast alloys (A356) [37,38] and with commercially pure Al (AA1230) [36]. However, alkaline-aluminates electrolytes are highly aggressive toward aluminum oxide, such that it is necessary to pre-coat the Al surface with a short aluminate-free PEO process before starting the actual PEO

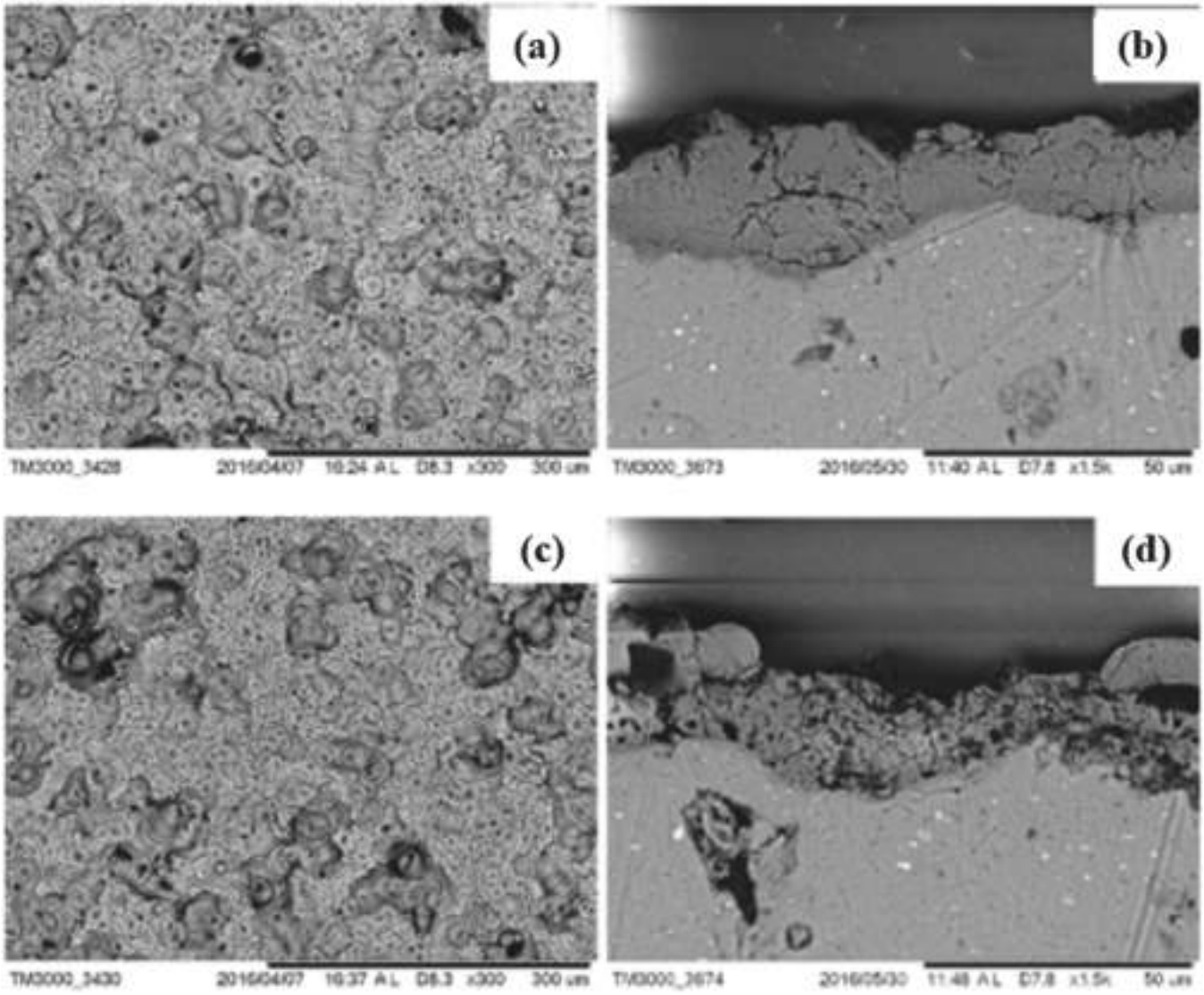

Fig. 5. SEM magnification of the surface and section of commercially pure aluminum PEO coated in: a), b) Na^+ containing electrolyte; c), d) K^+ containing electrolyte. Adapted from [23].

coating [38]. Furthermore, using aluminate requires the addition of NaOH to avoid their precipitation [38]. Fluoro-aluminates (Na_3AlF_6), instead, have been introduced during the PEO coating of AA6061, with an improvement in hardness and thickness [10].

Zhang et al. have used yttrium nitrate ($Y(NO_3)_3 \bullet 6H_2O$) as an additive during the PEO of AA2024 in a silicate-phosphate aqueous solution [39]. Its presence caused an increase in the coating growth rate and in coating hardness [39]. Furthermore, corrosion resistance has increased: the dissolved yttrium ions have formed yttria (Y_2O_3) and yttria-silica mixed oxides in the pores and cavities of the alumina matrix [39]. Thus, yttrium nitrate introduction has led to a porosity decrease, maximum at 1.5 g/L $Y(NO_3)_3 \bullet 6H_2O$ [39].

Cobalt salts, instead, have been introduced by Rakoch et al. in the electrolyte for the PEO coating of AA2024 for producing dark anticorrosion coatings, with a tone ranging from brown to black according to the coating thickness [40]. Another way of producing colored PEO coatings on an aluminum substrate is to introduce dyes or pigments in the electrolyte [8].

There are then other proposed additives, on which the knowledge is smaller and mostly referred to as commercially pure aluminium: they are K_2TiF_6, KF, and NaF [10]. About the last one, Egorkin et al. report that it is useful mainly in the earl of the process, contributing thanks to the oxidizing ability of F^- at substrate passivation [28]. Also buffering agents for limiting pH variations during the process might be introduced: one example is $Na_2B_4O_7 \bullet 10H_2O$ [28,41]. However, the presence of borax increases the breakdown potential in PEO treatments on pure aluminum [41].

There are then different examples of the addition of corrosion inhibitors in the electrolyte for increasing the corrosion resistance of the resulting coating [33], but they will be treated together with the functionalization processes of the PEO-coated surfaces.

5.1.8. *Effect of electrolyte impurities*

Anions such as chlorides or sulphates are impurities easily found in the electrolyte, originating from water, chemicals, or a not perfectly cleaned metallic surface. For AA2024 and AA1230, Terleeva et al. state that their major effect consists of a loss of process efficiency and coating growth rate. Thus, aspects different from the coating thickness and the energy consumption, such as microstructure, porosity, and composition are not affected by impurities. The reduction in thickness provided by their presence, however, can be estimated at -25%, even though this loss can be recovered by extending the process by 25%-30% of the time [36]. Furthermore, it has been reported also that an addition of sodium carbonate in the electrolyte can counteract the pollutant's effect, reducing

their damage [36].

5.2. Effect of the dispersed additives

Dispersed additives, such as microparticles or nanoparticles, are frequently encountered as electrolyte constituents in PEO of aluminum for various aims [1,3,8]. According to the kind of particulate used, the incorporation can either be mechanical or chemical, with the involvement of its chemical species in plasma-induced reactions [3].

In the first case, most of them are embedded in the outer coating layer, helping to decrease the pore's number and size, resulting in an improved corrosion resistance, adhesion, and hardness of the coating [2]. Also, their presence might modify the physical-chemical behavior of the coating itself [2]. For instance, PTFE particles added during the PEO of AA2024 alloy can make the coating chemically inert and increase its wear resistance, while alumina and zirconia nanoparticles incorporated during the PEO of AA7075 alloy are able to make the coating hydrophobic [2]. Particles with a 2D layered shape are considered to be more able to close the coating pores [42,43]. Xi et al. for instance, PEO coated AA2024 in a phosphate-based electrolyte containing a variable amount of quasi-2D sericite particles (average diameter 3.5 μm). SEM analysis revealed the creation of a "barrier network" of particles oriented almost parallel to the metal-coating interface [43]. As a result, the pathway for Cl^- and O_2 toward the metallic interface is made more complex, and corrosion onset is delayed [43]. Other carbon-based nanoparticles, such as nanotubes, graphite or diamond, have been tested as additives too, on different Al alloys. They all showed a beneficial effect both on the corrosion resistance, due to the porosity reduction, and on the wear resistance [44].

Hexagonal boron nitride (h-BN) nanoparticles, instead, are mechanically included in the coating during PEO on Al 2024, as shown by Li and Di, filling the pores and creating a solid lubrication effect [45]. Furthermore, they can enhance the coating corrosion resistance of one order of magnitude, even if in a too large amount they create segregates, decreasing coating compactness and protectiveness [42]. Basalt powder microparticles (< 5 μm) have been tested by Terleeva et al. during the PEO of AA2024 [46]. Their addition into a classical alkaline-silicate electrolyte has led to a large increase in the coating thickness, which reached 180 μm, with the basalt powder particles mainly concentrated in the outer layer [46]. Their presence noticeably enhanced the outer layer hardness, reaching 1110 HV, even though not up to the levels of the inner, alumina-based, layer (1850 HV) [46].

Liu et al. reported that the introduction of graphene nanoparticles during PEO of D16T alloy (analogous to AA2024) can enhance the transformation of amorphous oxides into crystalline alumina, improving hardness and corrosion resistance [47]. Graphite particles, instead, have been tested by Wu et al. by using an aluminate-based electrolyte [35]. In their presence, the α-to-γ alumina ratio decreases, but the pores get smaller. Furthermore, the coating gains self-lubricating coatings, showing a very low friction coefficient [35].

Other examples of particles added to the PEO electrolyte and inertly included in the coating are SiC, TiO_2, and MgO, usually for coating densification and wear resistance increase both with AA2024 or with other alloys [47]. There is an example of the use of Si_3N_4 nanoparticles too, even though on pure aluminum. Their incorporation however does not produce any improvement: in their presence, larger pores and cracks are obtained, and particles segregate in clusters over the surface [41].

The incorporation of particles in the PEO coatings is strongly dependent on the electrical parameters chosen for the process. Vakili-Azghandi et al. have reported that, for AC PEO on AA6061, higher current density and larger frequency lead to an increase in particles uptake [48].

On the other side, the literature about particle reactive incorporation during PEO on alloy 2024 is quite poor, while there are more examples concerning the PEO of other alloys, Al-, Ti- or Mg-based. Mojsilovic et al. have tried to incorporate during PEO of 2024 alloy some Zn-Al LDH particles (Layered Double Hydroxides) [49]. The PEO process destroyed LDH nanoparticles due to the too high temperatures reached into the sparks, but elements originating from LDH have been included, together with elements originating from the peculiar electrolyte additives used, such as Ti [49]. However, the resulting coating, enriched by titanium oxides and zinc-aluminum mixed oxides has shown enhanced corrosion resistance and photocatalytic behavior, normally not typical of alumina [49]. Silver nanoparticles too are able to participate in the plasma reactions [50]. Santos et al. have introduced them into a silicate electrolyte for the PEO of commercially pure aluminum. The obtained coating shows a small amount of Ag atoms in the ceramic structure, giving antimicrobial properties to the surface [50].

6. Effect of the electrolyte temperature

During PEO, an enormous amount of heat is released by the plasma sparks into the electrolyte, such that a cooling system is included in almost all the treatment units, even though precise control of the bath temperature is difficult due to the large gradient created within [34]. Previous papers reported different temperatures for the electrolytic bath, either above or below room temperature, even though its precise effect on the process has to be fully clarified yet.

Indeed, if in traditional anodizing low temperatures are required for achieving a good coating quality, the effect of process temperature on PEO coatings is more complex, and has effects on the resulting coating, on its properties, and also on the process itself [34]. By comparing PEO coatings obtained between 10°C and 80°C, Cheng et al. found that hot baths provide a decrease in the breakdown potential, and thus a thicker and more homogeneous final coating, even though poorer in α-Al_2O_3 than the ones produced at a temperature lower than the room one. Despite this, the high temperature coating showed a corrosion rate two orders of magnitude larger than the ones produced in a cold electrolyte [34].

7. Effect of the electrical input

A first classification of the electric regime can be done based on the control parameter of the cell, which can be powered both in current density control and in voltage control. In galvanostatic mode, while the current density is kept constant the potential to be applied by the power supply rises in time, due to the coating thickening which increases the breakdown potential. For this reason, discharges become larger in size, stronger in intensity, and more destructive [51]. During potentiostatic PEO, instead, Liu et al. [51] report that when the potential is kept constant for a long time the spark intensity decreases due to the same phenomenon, and also the current density measured does. Thus, sparks become colder and less violent. This can be grasped qualitatively just by looking at the light emission intensity curve reported in Fig. 6.

The control parameter (current or potential) can be then supplied in different modes (direct, alternating, pulsed) and with different histories (ramps, steps, breaks) [1]. This may influence the coating thickness and morphology, the structure, the hardness, and the porosity [2].

7.1. The role of the current regime

The main difference between using a direct (DC) supply or an alternating (AC)/pulsed one is that, with direct current or voltage, the intensity and the duration of the discharges increase with time, leading to destructive events and oxide or substrate deterioration [1,52,53]. Therefore, the coating becomes more cracked and less adhered to the substrate [53]. This does not occur with alternating/pulsed regimes, since at the end of the pulse, or of the half-cycle, the current flow is interrupted and the discharges stop before they can get destructive [1,2,9,52]. Thus, alternating or pulsed regimes are preferred for obtaining thicker, denser, and harder coatings [9,52,53]. As reported by Ceriani et al., PEO coatings produced in AC regime display a more regular

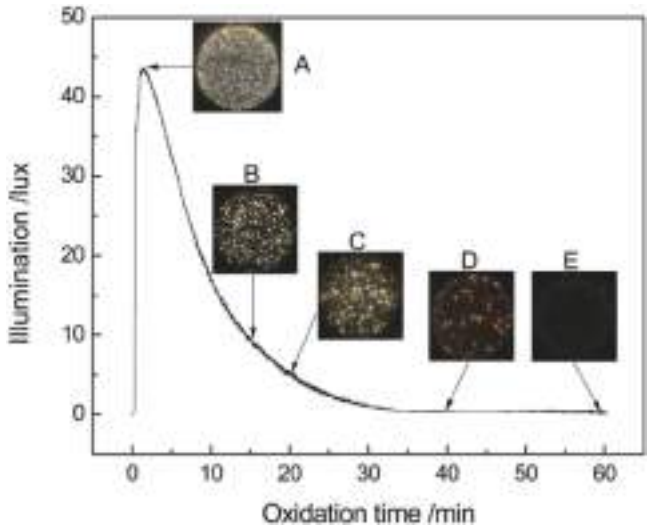

Fig. 6. Illumination intensity during a potentiostatic PEO process of AA2024. Adapted from [51].

morphology too, due to the lower size of the discharge craters on the coating surface [54]. Furthermore, AC PEO can offer lower energy consumption [55]. There are also some examples of "hybrid" current regimes, composed of a unipolar and a bipolar part, even though not on aluminum alloys [9].

Another power regime that is gaining more interest is the pulsed bipolar current, in which both cathodic and anodic pulses are supplied to the substrate [56,57]. Using a pulsed bipolar regime could bring improvements in the coating quality [57] and reduction of the porous coating growth [56]: Yerokhin et al., indeed, have reported a porous thickness between 10% and 15% with this waveform applied to alloy 2024 [57].

Finally, also more complex waveforms, originating from the superimposition of different waves, are encountering a wider diffusion. Du et al. [56], by using a linear combination of square waves, managed to suppress almost totally the porous layer of the coating on the AA2024 surface.

7.2. Time evolution of a PEO treatment

As mentioned above, in galvanostatic PEO the applied potential grows when the current is kept constant. The resulting voltage vs time curve (Fig. 7), shows four different stages, corresponding to different sparking modes:

1. Stage I: it is the beginning phase of PEO, where the passive film is created with a large gas evolution, not dissimilarly to a traditional anodizing process, and the sparking has not started yet,
2. Stage II: small discharges appear on the substrate metal, quickly traveling across the whole surface, while the voltage growth rate drops,
3. Stage III: usually called the "microarc" stage. Discharges become larger in size and slower in traveling around the surface, while the potential growth rate becomes even smaller,
4. Stage IV: the voltage growth rate goes on decreasing, and large, long-lasting discharges appear, with a destructive effect [2,58].

If operating in DC, thus, to avoid high-intensity destructive discharges it is necessary to move at lower current density (or potential) values [2]. This implies, however, a slower oxide growth [2]. For this reason, operating in an AC or pulsed regime is often preferred.

As Fig. 7b shows, even though the phases 1 to 4 have been defined for DC PEO, a similar evolution of the plasma discharges has been observed for AC PEO of aluminum alloys too [2,24].

7.3. AC and pulsed current PEO

Moving away from DC anodizing introduces new variables: the waveform and the frequency. In the past, most of the processes adopted 50 Hz-60 Hz sinusoids [3], even though in recent years higher frequencies are becoming more used. Furthermore, a period of cathodic polarization seldom involving cathodic sparking [1,3] is introduced too: its effects have been an object of copious recent studies.

7.3.1. Effect of the cathodic polarization

The application of cathodic polarization to the substrate, interrupting the anodic periods, appears to be beneficial for the coating [1,3]. Indeed, its quality and thickness increase not only if the cathodic half cycle is present, interrupting the spark growth, but also if the cathodic voltage raises [3,59], or if the cathodic polarization time becomes longer [60]. Xin et al. [53] proposed that the anodic current value can be related to the resulting thickness, while the cathodic current value can be related to the coating compactness. This agrees with the results on AA2024 of Li and Di [60], who stated that by increasing the duration of cathodic pulses concerning the anodic ones, the coating thickness decreases while its compactness, adhesion, and homogeneity are improved.

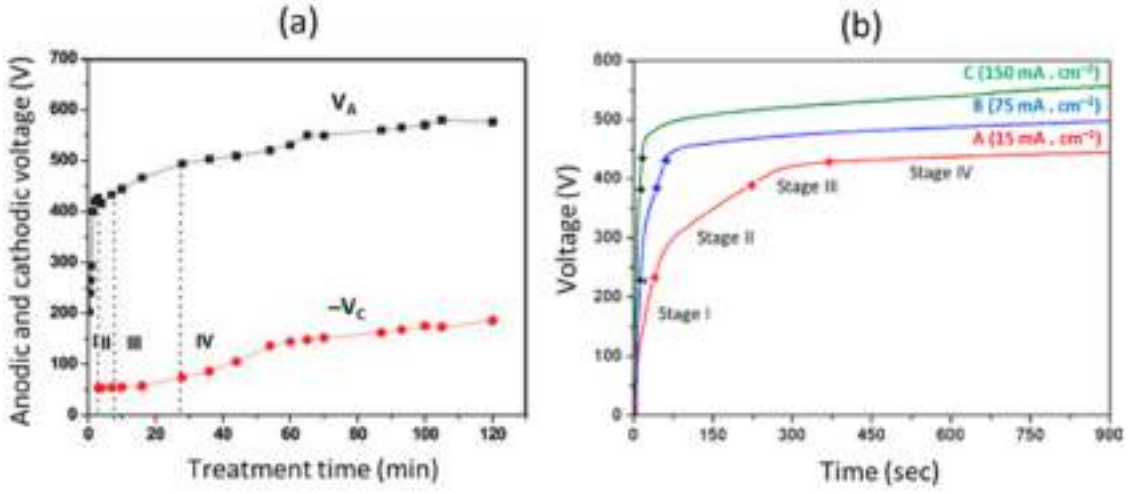

Fig. 7. Voltage-time curves of Mg alloys showing the four stages of sparking, obtained during a) AC PEO and b) DC PEO. Adapted from [2].

Rogov et al. [61] observed on AA2024 that the electric behavior of the oxide layer is different during cathodic and anodic polarization. During the first, the coated metal offers an inductive behavior, with a positive phase shift of the response from the stimulus, and its local resistance decreases, while during the latter the coating behaves as a capacitor, leading to a negative phase shift, and the coating resistance locally increases [55,61]. As a result, during alternate polarization the low resistance sites, where discharges are more likely to occur, move along the surface, thus increasing the coating homogeneity [55].

The occurrence of discharges during the cathodic half-cycle has been frequently reported, in particular in strongly alkaline electrolytes, where proton shortage might hinder the hydrogen evolution, usually expected at the cathode [3]. Even though the charge transport mechanism during cathodic discharges is still unclear, they are likely to contribute to the coating growth [3,52].

It has been reported, however, that reaching the breakdown in cathodic polarization is more difficult than during anodic polarization [3]. The reason for this difference could be found in the fact that during anodizing the limiting step for charge transfer is ion movement in the electrolyte [3]. During anodic polarization, the OH^- ions are moved toward the surface, while during the cathodic half-cycle, the H^+ ions are pushed toward the surface. There, they accumulate in a capacitive structure called an electronic double layer (EDL) until charge storage is high enough to allow oxide breakdown [3,62]. Since hydroxyl ions move much slower than protons, electric conduction through the oxide will be slower during anodic polarization, thus determining a stronger electric field across it, leading to the breakdown [3].

Cathodic discharges might take place in the same locations where an anodic discharge occurred, due to the less protective oxide layer formed there [52]. However, this occurs only if there is enough time after the anodic discharge for filling again the discharge crater with the electrolyte, [3]. Thus, if the frequency is large enough, anodic and cathodic discharges will take place at different sites [3]. Conversely, it is more difficult to observe the concentration of anodic discharges where a cathodic discharge occurred [52]. Indeed, according to the mechanism illustrated in Fig. 8, cathodic discharges produce a nanoporous layer of hydrated alumina which, after the following anodic breakdown is changed into a compact layer, highly resistive, hindering the occurrence of other breakdowns [52]. As a result, anodic breakdown sites are randomized, and the possibility of having localized, long-living discharges is hindered, decreasing the total porosity of the oxide [52]. This

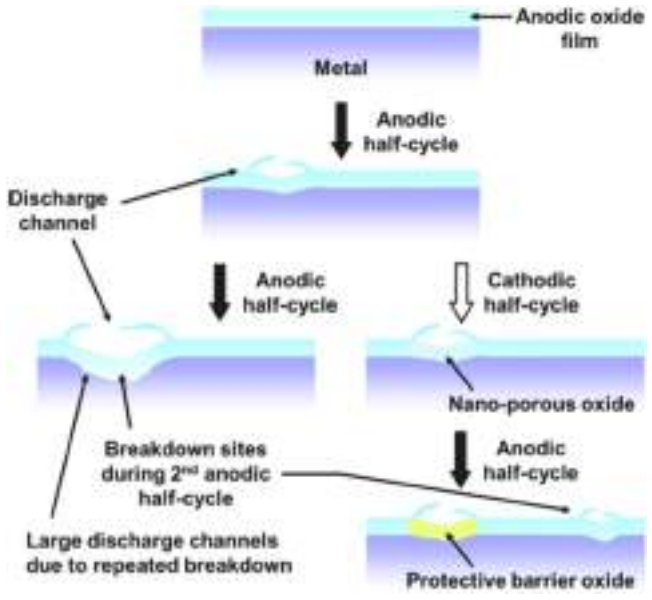

Fig. 8. Schematic illustration of the microstructural changes led by the anodic and cathodic cycles to the discharge sites. Adapted from [52].

mechanism leads to an increase in coating compactness, so it can be said that while anodic discharges mainly contribute to increasing thickness, oxidizing new metal, cathodic discharges contribute to enhance the coating quality, re-melting the oxide in a more compact morphology [53].

7.3.2. *Main parameters in AC PEO*

In AC (or pulsed current) PEO as in DC, the voltage (or the current density) applied is the main variable determining the resulting coating thickness [9,59]. Yan et al. reported that the final thickness increases with the applied current density, even though the maximum corrosion resistance on AA2024 is obtained at 15 A/dm^2, above which the defect density becomes too high [63]. Furthermore, a higher current density helps alumina crystallization into the α and γ forms, due to the higher plasma temperatures [63]. Maximum surface hardness, instead, is obtained at 20 A/dm^2 [63].

There are then other parameters more typical of AC PEO, such as the ratio between anodic and cathodic current, the frequency, or the duty cycle. Student et al. indicated 15:10 as the optimal ratio between anodic and cathodic current density for achieving fast oxide growth on an AA2024 substrate [26].

Frequency has a key role in determining the discharge lifespan since the end of the anodic half-cycle stops all the ongoing discharges [3]. At 50 Hz – 60 Hz, the waveform period is long enough for the development of a long spark cascade, thus of a large quantity of oxide. However, frequencies around 1000 Hz – 1500 Hz are becoming popular since they allow for obtaining shorter discharge events leading to a finer microstructure, with smaller porosities, even though with a slower growth [3,59]. Higher frequencies, with a period comparable to a single discharge lifetime (thus, around 2000 Hz) promote instead the rise of cathodic discharges, as reported by Clyne and Troughton [3,59].

The duty cycle, i.e. the ratio between the on-time and the total anodizing time, influences the coating quality [59]. A high duty ratio reduces the breakdown voltage [41] and facilitates the oxide growth but produces also a more porous and cracked coating than the ones obtained ad low-duty cycles [59]. The final coating thickness, however, seems to be only a function of the applied voltage, while frequency and duty ratio mostly control the coating quality [59].

Finally, it must be considered also that the features of a PEO coating depend not only on the single electrical parameters but on how they can interact [59]. An et al. have reported that for achieving a maximum coating growth rate the best combination is high voltages, low frequencies, and large duty ratios. However, the best corrosion resistance has been observed for specimens anodized at lower potentials, high frequencies, and small duty ratios [59]. Furthermore, the effect of the electric regime cannot be studied by itself, since it is always connected to the electrolyte used [1].

8. Effect of surface pre- and post-treatments

The highly porous morphology of the outer layer of the PEO coatings offers the possibility of applying several post-treatments to change the surface microstructure and its properties after anodizing. Sealing treatments are the most documented, meant to decrease the coating porosity, thus improving its corrosion resistance [28]. Furthermore, the pore sealing process could be exploited also for altering the surface chemical and physical behavior, changing for instance its wettability, its friction coefficients, or loading its pores with corrosion inhibitors.

The literature about surface pre-treatment is instead quite poor, even though a few examples are given in the following paragraphs.

8.1. *Surface post-treatments*

Most of the PEO post-treatments reported for AA2024 involve the clogging of the coating pores, even though adopting different strategies, sometimes involving also the loading of the coating with corrosion

inhibitors. One of the most reported sealing processes is the deposition of polytetrafluoroethylene (PTFE) by vacuum impregnation into the coating pores, to seal them [28,64,65]. This allows an enhancement of the barrier properties, thus an increased corrosion resistance [28]. Furthermore, since PTFE particles act as solid lubricants, their presence does not bring only a mechanical pore occlusion, but it can enhance the surface tribological properties too [28,64,66], for instance by reducing the wear rate [64]. Lu et al. suggested that for maximizing the wear resistance of the PTFE sealed coating it is recommendable to perform PEO at high potentials, to increase oxide roughness thus favoring particle penetration during sealing [64]. The best wear reduction has been reported for a 40% surface density of micro-cavities [66], even though such a configuration shows a low surface hardness [66].

A weak point of PTFE sealing, however, is the UV-induced degradation of the sealed layer, with a consequent reduction of electrochemical and mechanical properties, which becomes evident during field exposure testing [28]. However, Egorkin et al. have measured on PTFE-sealed coatings a polarization resistance value of two orders of magnitude higher than on an AA2024 PEO coating even after UV exposure and marine exposure. The effect of PTFE sealing on corrosion resistance can be observed also in the surface aspect of the specimens after exposure, as given in Fig. 9 [28].

Li and Di have proposed an alternative polymer-based sealing process for PEO coatings on AA2024, involving the immersion in molten paraffin, which fills the pores and the cracks, and once solidified, offers a self-lubricating effect [70].

Another pore sealing strategy, seldom adopted, is to fill the pores with corrosion inhibitors, especially when an increase in corrosion resistance is required [65,67]. Immersion tests in artificial seawater conducted by Oleynik et al. evidenced that pore filling with commercial organic-based corrosion inhibitors can delay the appearance of localized corrosion defects, even though the longest time to corrosion onset has been shown by sealed specimens onto which a top PTFE layer was applied [65].

An alternative strategy for sealing the PEO coating porosities is to chemically transform the outer coating layer, growing expansive products in the pores and over the surface. An example is the synthesis of a ZnAl layered double hydroxide (ZnAl LDH) upon PEO coated aluminum 2024 specimens reported by Liu et al. [68]. By exposing the coating to an aqueous solution of zinc nitrate at 90°C for 12 h, its surface is covered with a complex network of LDH flakes covering the porosities. Furthermore, this peculiar microstructure has self-healing behavior and favors the intercalation of corrosion inhibitors such as vanadate and molybdate, further enhancing the corrosion resistance [68]. The protective layer thus obtained exhibits high stability also in aggressive environments such as simulated seawater, where the coating polarization resistance starts decreasing only after 20 days of immersion [68].

Sol-gel treatments have been considered for PEO coating sealing too [67]. Akbarzadeh et al. built a sol-gel sealing layer upon AA2024 specimens PEO anodized and loaded with corrosion inhibitors, using GPTMS and TEOS as precursors, dissolved in ethanol [67]. Del Olmo et al. applied a sol-gel sealing using the same precursors but loading them with SiO_2 nanoparticles for coating densification and with Ce^{3+} salts for corrosion inhibition [69]. In both cases a good adhesion of the additional layer, a reduction of roughness and a corrosion resistance improvement was observed [67,69]. The presence of Ce ions allowed corrosion protection even in the coating defects and in harsh conditions such as seawater immersion [69].

Fig. 9. (a) Bare, (b) PEO-coated, (c) PEO-coated and sealed AA2024 after 30 days of simulated marine exposure. Adapted from [28].

Wang et al. have proposed for alloy 2024 to seal the pores and the cracks by epoxy resin impregnation. In this way, a synergistic effect between the ceramic matrix and the impregnated resin has been observed, resulting in enhanced fatigue resistance of the alloy. Filling the micro-defect, indeed, removes sites where stress concentration occurs, thus delaying crack initiation and propagation [70].

Other proposed post-treatments for PEO-coated aluminum alloys involve chemical vapor deposition (CVD) of fluorinated compounds upon the PEO coatings to increase the water contact angle, making it superhydrophobic, thus enhancing its corrosion resistance. However, the durability of the resulting layers seems to be scarce [71].

8.2. *Surface pre-treatments*

If the literature about surface post-treatments after PEO is quite rich, the one about surface pre-treatments before PEO is, on the contrary, quite poor. Only a few examples are available for aluminum alloys.

Gu et al. have studied the effect of the roughness and the grain size reduction by ultrasonic cold forging (UCFT) of AA2024 surface before PEO. This treatment leads to an enhanced quality of the ceramic coating, which shows a smaller porosity, a higher hardness, and a higher corrosion resistance if compared to the one obtained on a non-pretreated surface [72].

Another possible mechanical pre-treatment before PEO is shot peening, performed by Asquith et al. for improving the fatigue life of ceramic coated AA2024 components [73]. The fatigue life of the specimen increases by 85% with respect to the ones treated only with PEO, because of the compressive residual stresses induced by the surface pre-treatment [73]. The effect of shot peening on the corrosion resistance of the PEO coated alloy is instead more controversial. Wen et al. have tested by long-time immersion in simulated seawater (3.5% wt. NaCl) a PEO coating grown on AA2024 whose surface underwent an intensive shot peening (SMAT, Surface Mechanical Attrition Treatment) [74,75]. The pre-treatment succeeded in forming a 20 μm surface layer with nanosized grains (average size 53 nm), which did not show any growth during PEO due to the low heating of the substrate [74,75]. However, the PEO coating proved to be more porous than the one formed on a non-pretreated sample, mainly because of the multiplication of the discharge sites due to the introduction of defects. As a result, the shot-peened surfaces showed a lower corrosion resistance than the non-shot-peened ones, even though in long-time immersion their polarization resistance appeared to increase thanks to the formation of a denser passive at the metal-electrolyte interface [74].

Iqbal et al. applied traditional anodizing on AA2024 as a pretreatment for PEO. They observed that such a precursor allows for a reduced energy consumption during PEO and helps obtaining the sparks softening. Corrosion resistance and coating properties, instead, were not affected by it [76].

Fan et al., instead, have built a PEO coating on a laser-textured aluminum surface. Firstly, they produced a regular line pattern with a 100 μm pitch (Fig. 10a). Then, they PEO-coated the textured surfaces with different AC voltages and treatment times. Fig. 10b shows that the pattern of the substrate is quite well reproduced on the coating. Furthermore, the PEO oxide thus obtained appears to be more adherent than the one produced on a flat surface [77]. Furthermore, laser-based pre-treatments have proved to be beneficial also for the quality of the PEO coating: indeed, the fast melting and solidification induced by the laser beam leads to a decrease in number and size of the intermetallic particles, leading to a lower number of defects in the coating [78].

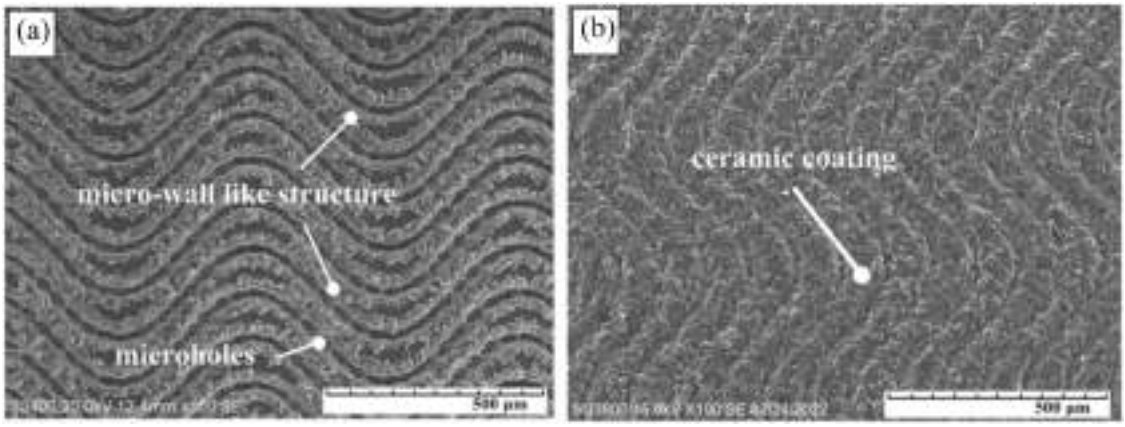

Fig. 10. A laser-textured Al 2024 surface (a) before and (b) after the PEO coating. Adapted from [77].

9. Plasma discharges and coating growth

9.1. Onset, evolution, and extinction of a discharge

As soon as the PEO process starts, and the thin dielectric film forms over the metal surface, the electrical resistance rises, thus requiring an electric field strength increase for keeping the current set, if the process is run under current control [1,2]. The passage of a current, however, determines the creation of a gaseous film, originating from electrochemical reactions, on the metallic surface. This further increases the resistance, requiring a new potential enhancement [1]. After a certain time, the electric field is strong enough to activate the dielectric breakdown, thus initiating the plasma discharge [1,2] at the bottom of a pore, where the dielectric thickness is lower (Fig. 11a) [3].

This mechanism thus encompasses a delay between anodic polarization application and discharge onset, which might range from some hundreds of nanoseconds up to a few milliseconds. This depends on the fact that breakdown can occur only when charges accumulated at the oxide-electrolyte interface (which form the EDL, Electronic Double Layer) exceed the charge storage capacity of that interface. Thus, rougher and porous oxides are expected to increase this delay, due to their large specific area associated with a high charge storage capacity [62]. Also, operating PEO in AC mode increases this delay since cathodic polarization moves away the charges from EDL. Thus, during the subsequent anodic polarization, a longer time will be required to build up enough charge for oxide breakdown. Thus, the longer the cathodic polarization, the longer the delay for discharge onset [62].

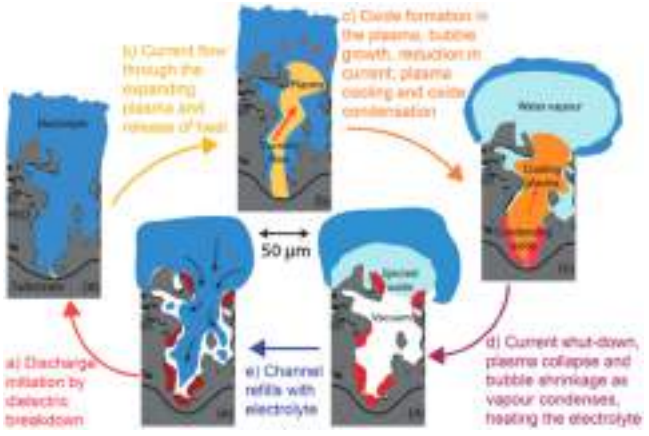

Fig. 11. Illustration of the phases of a plasma discharge: a) discharge triggering at the bottom of a pore, b) discharge channel creation, c) the water vapor bubble grows, d) current shut down and oxide condensation, e) pore re-filling with electrolyte. Adapted from [3].

During the breakdown, electrons are injected at the electrolyte/gas interface, and a discharge channel forms, crossing the whole oxide thickness (Fig. 11b) [1]. Substrate cations migrate outward, and oxygen ions migrate inward within this micrometer-sized [3] channel, as established by the direction of the applied electric field [1]. As they meet, they form substrate metal oxide [1,3]. On aluminum alloys, local current densities of the order of magnitude of several kiloamperes per square centimeter have been measured [1], with electron densities between 10^{15} and 10^{18} cm^{-3} [3]. The channel temperature is between 8000 K and 10,000 K [3,79]. The energy brought by a single discharge can be estimated at around 1 mJ [3]. If these high temperature plasma phenomena lead to a great heat release in the bath, on the other hand, temperatures larger than 120°C have never been registered inside the aluminum substrate. Thus, no significant microstructural alterations have been never reported [34,51].

The extinction of the single discharge is caused by a fast resistance increase in the discharge path. This is not due to the oxide growth, much slower, but to the development of a gaseous layer at the top of the discharge channel (Fig. 11c) [3]. During the discharge, the electrolyte surrounding the discharge site is heated and vaporized, creating a relatively cold (2000 K [79]) bubble of water vapor containing also some electrolyte solutes [3]. At first, this bubble is small enough to have a good concentration of ions in it, thus allowing electric conduction. Then, it grows quickly by incorporating new vapor, and the ions become more diluted, decreasing the conductivity of the discharge path. Thus, resistance increases both because of this effect and because of the increase in the bubble dimensions. As soon as the bubble is large enough, the current stops, and plasma cools down forming again the oxide-electrolyte interface (Fig. 11d) and leaving the site for a subsequent discharge (Fig. 11e) [3]. According to most of the literature sources, substrate atom oxidation occurs while the plasma cools down. During this period, the freshly formed metal oxide condenses into a liquid and deposits on the channel walls [2,3].

9.2. Cascades of discharges

The duration of a discharge event is usually in the range of microseconds, which is a too short interval for being perceived by the naked eye. However, the individual discharges occur in cascades of tens or hundreds in the same location, thus becoming visible [2,3]. The local morphology of the surface determines preferential locations where a cascade can be hosted: for instance, deep pores, having a smaller dielectric thickness, might stabilize them [3]. The end of a cascade is determined by the growth of the molten oxide generated, which locally increases the electrical resistance, making a breakdown in a nearby site. Between two cascades, an incubation time of some milliseconds is

observed [3]. However, it must be remembered that, if PEO is operated in AC, the duration of the discharge events is limited by the end of the waveform half-cycle [3]. After the end of the breakdown, if the PEO is performed in AC mode, during the cathodic half period the metal oxide undergoes relaxation phenomena, and a part of the oxidized species could get reduced [2].

At the beginning of the PEO, the sparks are small and located where the electric field is stronger on the surface (Fig. 12a-b) [1]. Then, cascades grow in dimension and duration, becoming more energetic, but lower in number (Fig. 12c-d) [1,3]. Larger discharges dissipate more heat, leading to higher heating of the discharge channel boundaries and the nearby regions. This promotes the crystallization of the molten oxide as α-alumina, the phase transformation of the surrounding oxide to high temperature phases and facilitates the onset of new discharges near existing ones [1].

9.3. Classification of discharges

By means of Optical Emission Spectroscopy (OES), it has been possible to study the features of the discharges in the different phases of PEO. Hussein et al. first proposed a classification of them based on their characteristic and their location [79]. Then, different authors have used this classification in their works, also identifying other kinds of discharge [24,58]. The systematization thus obtained comes mainly from works conducted on commercially pure aluminum, even though its accuracy has been proved for aluminum alloys too. The main discharge types, illustrated in Fig. 13, are [24,58,79]:

- Type A, originating from the top coating or the gases upon the specimen surface, produce electrolyte elements incorporation,
- Type B, originating from the substrate/coating surface, create a large discharge channel [51] and lead to substrate oxidation,
- Type C, originating from the coating defects, lead to electrolyte elements inclusion and porosity reduction,
- Type D, originating from the macropores, increase the inner layer thickness,
- Type E, strong and confined to the outer coating layer, leads to its densification.

Discharge types A, B, and C are common during traditional PEO processes, while types D and E are encountered more frequently during soft sparking phenomena [24,58], which are the object of the following paragraph.

The representation of Fig. 13 is slightly controversial since Liu et al. affirmed that every spark, irrespective of its initiation place, creates a discharge channel crossing the whole oxide thickness, at least during the final phase of its life [51]. According to them, indeed, it would not be possible to have any kind of electrical conduction through an alumina-based coating because of its high resistivity [51].

The discharge classification holds for both the potentiostatic and the galvanostatic PEO process, even though Liu et al. have noted that in the case of potential control, only discharges of A and B types are observed [51]. Small type A discharges are typical of potentiostatic PEO at its early phases and at very long times, while type B discharges are more commonly encountered in the middle of the process when the electron temperature is higher [51].

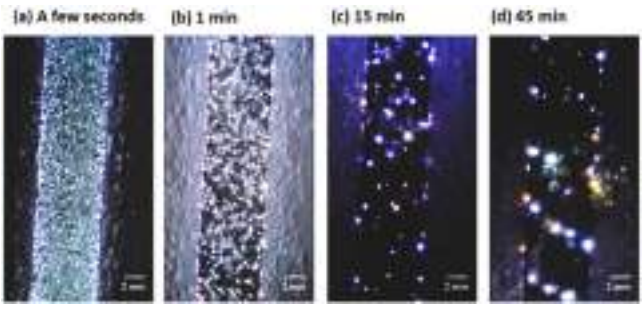

Fig. 12. Evolution of the aspect of the plasma sparks during the AC PEO of an aluminum alloy series 2xxx. Adapted from [80].

9.4. Soft discharges

Even though in AC mode some issues of violent and destructive sparking typical of DC PEO can be avoided, as the coating thickness grows the through thickness discharges become more intense and long-lived, imposing a limit to the achievable thickness [3]. However, the onset of these discharges can be avoided by operating in some specific conditions able to trigger a new kind of plasma regime, which is called "soft plasma" or "soft sparking", able to grow the coating thickness and improve its morphology [3,7,61]. This transition is observed only in the presence of dielectric oxides, thus only on Al and Mg, while not on Ti, being its oxide semiconductive. The cause for this is that the processes leading to the transition to soft sparking require prevalently ionic conduction, which would be suppressed by electronic conduction in semiconductor oxides [81].

As soft discharge appears, the sparks lightness and the acoustic emission drop (they become almost invisible and silent), and the potential, in current control mode, decreases: hence, the name "soft" sparking [7,23,24]. Furthermore, the distribution of the discharges on the specimen surface becomes more uniform [7]. Rogov et al. have also observed a decrease in oxygen evolution on AA2024 after the transition to soft PEO [61]. During soft sparking, the oxide growth rate increases, and the coating porosity reduces [7,23,24]. The resulting coating, shown in Fig. 14a, is still three-layered, but with a thicker compact layer [7,24,61] richer in α-alumina [24]. Thus, coating properties result enhanced, with increased hardness, smoothness and adherence [7,23].

For aluminum alloys, the main condition for observing the transition to soft sparking is to have an anodic to cathodic current density ratio (termed R) lower than one [7,61]. Most of the studies report a cathodic current density 20%-35% larger than the anodic one: a wider difference might lead to plasma extinguishment and interrupt the oxide growth [24]. Then, also high frequencies, high current densities and aged electrolytes might help this transition [3].

Different mechanisms, often non-consistent with each other, have been proposed for explaining the effects of soft sparking, thus, a larger amount of work is required to understand its exact mechanism [7,61].

Rogov et al. have proposed the concept of "active zone" for justifying the transition to soft sparking on AA2024 [7,61]. This zone is defined as the portion of the coating thickness in which the combination of aluminum cations and oxygen anions occurs, generating new oxide [7]. Since a strong electric field is required for this process, the active zone must be located in the deepest part of the coating [7,61], where Al^{3+} is directly provided by metal oxidation and O^{2-} arrives by diffusion through the fine porosities of the inner compact oxide layer [7]. The remaining part of the thickness is called the "product zone" [7]. The active zone, thus, almost coincides with the dielectric barrier layer, where discharges are ignited [61]. Rogov et al. reported that when, such as in soft sparking, the cathodic current dominates, the active zone results enriched in hydrogen complexes, formed by protons attracted there during negative polarization [7,61]. Their presence increases oxide conductivity, thus narrowing the extension of the actual barrier layer. Therefore, the barrier potential to plasma discharge is decreased, and discharges soften [7,81].

Another justification for the peculiarity of soft sparking can be found in the appearance of different types of discharge, as reported by other authors. Indeed, if types A to C are typical of traditional PEO processes, they are less intense in soft sparking [24,58], during which types D and E frequently occur [24].

Zhu et al. have pointed out the existence of another kind of discharge phenomenon, called chain-like discharges, and characterized by

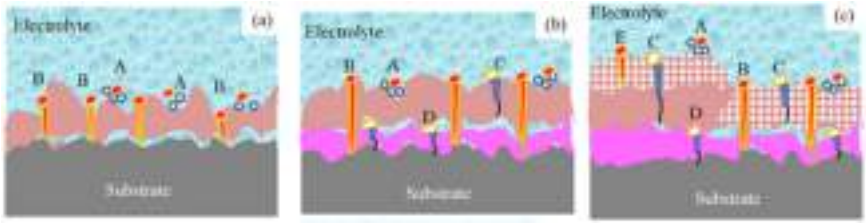

Fig. 13. Illustration of the different discharge types and their occurrence during a) phase I, b) phase II (micro-arc), and c) soft sparking. Adapted from [58].

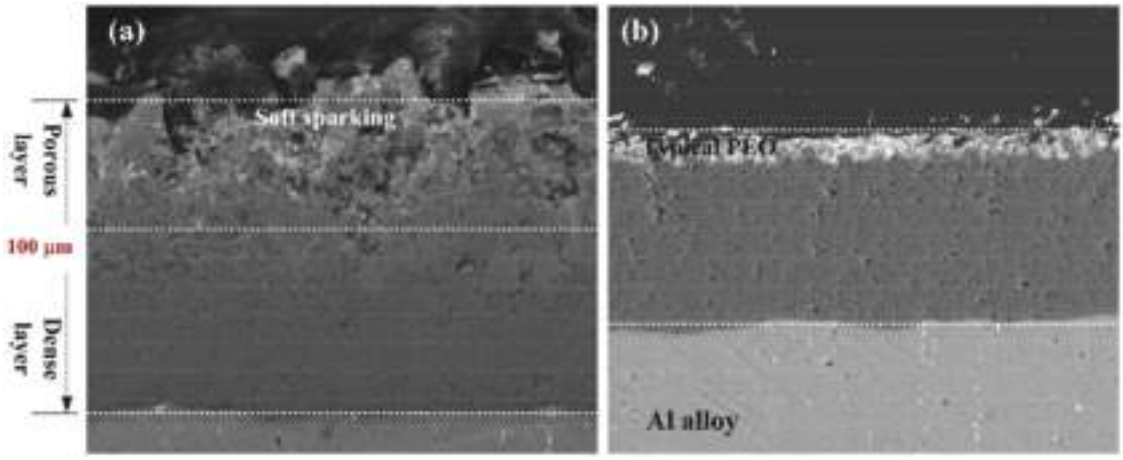

Fig. 14. Morphological differences between (a) a PEO coating obtained by soft sparking on Al and (b) one obtained by conventional PEO. Adapted from [24].

elongated chains of sparks crossing the whole specimen surface and arising at very long treatment times, after the soft sparking phenomena. This new kind of spark, shown in Fig. 15, leads to the transformation of the porous layer of the coating into compact oxide, thus producing a single, dense and defect-less coating layer [58]. However, no other occurrences of this phenomenon have been found in the literature.

9.5. *Kinetic of coating growth*

The kinetic of PEO coating growth is another aspect on which there is still a quite small literature. Shchedrina et al. have suggested that the AC PEO of AA2024, when operated at a constant current density, can be divided into two linear phases based on the oxide growth rate [82]. In the first one, the coating produced is highly porous, nonprotective, and

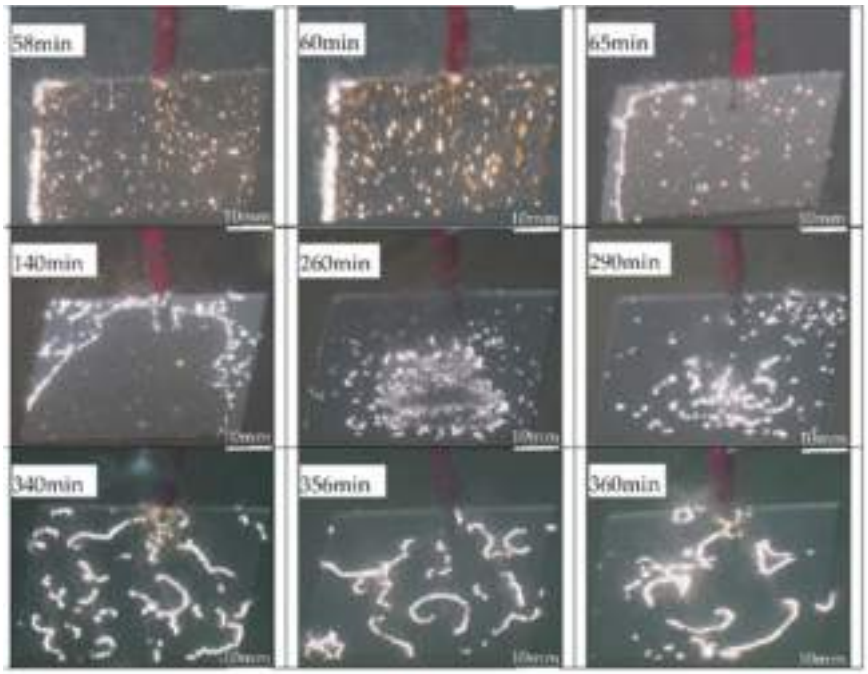

Fig. 15. Sequence of images of PEO on AA1060 alloy, showing the transition to soft sparking (58 min to 65 min) and the onset of chain discharges (260 min to 360 min). Adapted from [58].

shows a low adhesion. In the second phase, the coating thickness grows quickly, while the sample thickness is almost unchanged, meaning that the coating porosity decreases because of pore filling with freshly formed alumina [82]. The result is the formation of a compact layer in the inner part of the coating, while the outer layer remains porous. This second stage leads to the achievement of high hardness and corrosion resistance and can be related to the appearance of microarcs on the surface [82]. If soft sparking conditions are met, then, as reported by Zhu et al., a third and a fourth growth phase can be identified, during which the inner layer grows more rapidly than the outer one [58].

The increase in thickness or the compaction of the coating might be monitored during an AC PEO by acquiring the voltage and current waveforms during the process. Since oxide-based coatings display capacitive behavior, input and output are out-of-phase. This implies that, at a certain point of the anodic half-cycle, current stops at a not null potential, called threshold voltage: an increase in this value indicates an increase in the phase shift. This means that an increase in thickness or a decrease in defectiveness has occurred, determining a stronger capacitive behavior [1].

The oxide composition too evolves during the PEO process. Rogov et al. have reported that, during the initial stages of PEO on AA2024, the coating is mainly formed by oxidation of substrate atoms (Fig. 16a), while in the following more elements coming from the electrolyte are included (Fig. 16b) [14]. Thus, the initial stages of PEO can be described as an oxidation reaction, then, as the thickness grows, it shifts to a deposition from the electrolyte, and microdischarges move from the substrate interface to the coating one [14]. This transition is evidenced by the appearance of dark inclusions of copper oxide in the coating (Fig. 16b), which then compact into a dense layer (Fig. 16c-d) [14]. The newly formed alumina is mainly γ-alumina, which is metastable but needs sufficiently long exposure to high temperatures to transform into α-alumina, more desirable. This transformation, thus, becomes possible in the inner part of the coating when the coating is thick enough, so that the outer oxide plays the role of thermal insulation, ensuring a long enough high temperature time span in the inner coating [14].

9.6. *Coating homogeneity and current density distribution*

One of the main challenges in PEO is to obtain a homogeneous distribution of the coating thickness on the whole specimen substrate, especially on complex-shaped ones. Thus, it is essential to achieve a homogeneous current density distribution. The latter is controlled by two orders of parameters, thus generating a primary and a secondary current density distribution [55]. The geometrical features of the anodizing cell belong to the first class: thus, the first choice for addressing coating uniformity issues is to change the setup geometry, especially the cathode shape and its distance from the working electrode. The cathode-anode distance generates local inhomogeneities since more intense current pulses are registered in the regions of the workpiece closer to the cathode [2,55,83]. Wei et al. observed that current decreases as the anode-cathode distance increases when the anodizing potential is kept constant, until reaching a plateau value. This can be attributed to the ohmic drop into the electrolyte, directly proportional to the distance between electrodes [83]. This entails that different faces of the same working electrode would experience a different coating growth: the one closer to the counter electrode, as reported by Wei et al., will be thicker and more resistant to corrosion and wear [83].

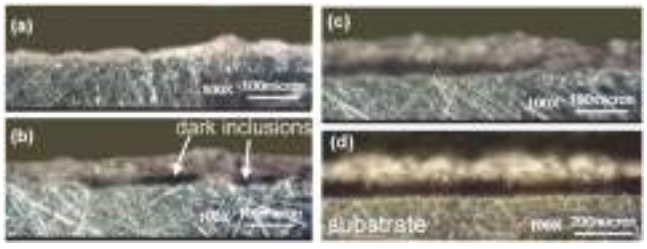

Fig. 16. Coating growth on AA2024 in subsequent phases: a) thin substrate oxide layer, b) dark inclusions of alloying elements and incorporation of electrolyte solutes c) and d) formation of the dense layer of copper oxide. Adapted from [14].

The cathode shape might be accommodated as much as possible, but, excluding massive production, having a specific cathode for every specific workpiece appears to be non-feasible [55]. Rotating the working electrode or increasing its distance from the cathode would instead improve coating homogeneity at a lower cost [83]. Then, it is possible to work easily on the secondary current density distribution. On this aspect, there is still a lot of work that can be done. It has been reported that increasing the alkali species in the electrolyte and decreasing the silicate concentration helps obtain more homogeneous coatings [36]. Another way of modulating the plasma for achieving better coating homogeneity is to add discharge softeners, such as organic acids [19, 32]. The electrolyte aging plays a role too, since nonuniform features have been observed more frequently after PEO performed with already used electrolytes [55], such that it is a quite common practice in large-scale PEO to "correct" the used solution by adding the chemicals consumed in the coating formation [36]. However, this practice is not able to clean up the electrolyte from residuals of the previous PEO processes [36]. Finally, Rogov et al. have reported that more homogeneous coatings with a smoother current distribution can be produced by inserting trains of cathodic pulses into the electrical input during the AC (or pulsed current) PEO of AA2024 [55].

10. PEO coating structure and composition

The PEO process, as previously mentioned, produces a three-layered coating, growing both inward and outward the original substrate shape [1]. The inner layer has a nanometrical thickness, it is amorphous [84] and defect-less, thus, it is usually named "barrier layer". Then, the intermediate layer is rather compact and crystallized, while the outer one is more porous, less adherent and it is the thickest one (up to 40% of the total thickness [4]). It is seldom called "technological layer" [1,4].

The quick solidification of the oxide brings a complex, highly disordered microstructure, characterized by a quite fine grain size [2,3], even though adjacent following discharges might induce some thermal treatments onto the existing oxide, with a consequent grain growth [3].

Nie et al. reported that from TEM observations it is possible to distinguish different sublayers into the barrier layer, all of them amorphous or poorly crystallized [84]. The intermediate layer, instead, is polycrystalline with gradually increasing grain size, and its lower portion is composed of nanoscaled crystalline grains [84]. Despite its compactness, also this layer hosts some micro-cracks and small flaws [1]. The technological layer, finally, presents large grains and a rather complex architecture of pores [3]. This might represent an advantage or an obstacle according to the properties required. Pores, especially the coarser ones, are a weak point for corrosion resistance and reduce the surface hardness so that it could be necessary to seal them [1,2], but, at the same time, they offer the possibility of functionalizing the outer layer, they increase the surface area and they enhance the coating strain tolerance [2,3].

The outer surface of a PEO coating presents a characteristic volcano-like crater morphology due to the peculiar mechanism of coating growth, involving the flow of molten oxide outside the discharge channels [2,4]. The surface roughness of PEO coated AA2024 specimens increases with coating thickness since thicker coatings produce stronger discharges, thus larger channels and craters [85].

Due to the rapid cooling of the molten oxide, the PEO coatings of aluminum alloys will present not only the stable α-alumina but also the metastable γ, ε, and η phases, in addition to amorphous phases [2,3] and mixed oxides coming from the substrate alloying elements or from the

electrolyte [10]. For instance, mullite is often found in PEO coatings since high silicate electrolytes are very popular for PEO of aluminum alloys [10]. These electrolyte-incorporated elements are more often found in the technological layer together with fused α-alumina, while the intermediate layer is made of a mixture of α- and γ-alumina [4]. Of course, it is not possible to heat treat the coating after its production to induce phase transformation since this would require temperatures much larger than the Al melting point [3].

11. Tribological and mechanical properties of PEO coated AA2024

Different authors report a high adhesion of the PEO coatings to the substrate [1,2,3], even though measuring it is not trivial. In particular, it has been reported that on aluminum alloys they are much more stable than on other valve metals such as Mg or Ti [1]. Terleeva et al. proposed to quantify it by measuring the extent of the defects appearing after a Brinell hardness test. On an AA2024 substrate, thinner coatings (< 100 μm) showed coating detachment in 4% of the indentation area, while thicker ones (> 100 μm) detached in 25% of the tested area [86]. Thus, coating adhesion seems to increase by decreasing thickness [86].

Because of the high adhesion, and other tribological features such as high hardness, low friction coefficient and high resistance to spallation, PEO-coated Al shows a reduced wear rate during service [2,3] and a high resistance to erosion in contact with fluids [86]. Furthermore, Ding et al. reported an enhanced resistance to fretting, even though higher in rainwater than in seawater due to a negative synergistic effect between wear and corrosion [87]. A PEO coating on a series AA2xxx might reach a hardness three to five times higher than the corresponding hard anodized coating [4], with higher hardness measured where the content of α-alumina is larger [10]. The friction coefficient, furthermore, gets even lower if the pores are filled with a solid lubricant sealant, such as PTFE or MoS_2 [4]. A low friction coefficient (0.52) has been obtained on PEO coated AA2024 by introducing 2.5 g/L of hexagonal boron nitride nanoparticles in the electrolyte [45]. An increase of the friction coefficient up to 0.85, instead, has been induced on the same alloy by incorporating basalt mineral powder during the coating process, as reported by Terleeva et al. [46].

PEO coating of AA2024 usually leads to a contact angle decrease, meaning a higher surface wettability with respect to the bare alloy (Fig. 17a-b) [47]. This justifies the great interest in pore sealing with hydrophobic substances, such as PTFE or graphene, both during PEO or in the post treatment. For instance, Liu et al. managed to decrease the hydrophilicity of PEO coatings on alloy AA2024 by introducing graphene in the electrolyte, obtaining a higher contact angle also with respect to the bare surface (Fig. 17c) [47].

The effect of PEO coating on the fatigue resistance of the substrate appears to be an important point, especially where AA2024 is chosen for its high load-bearing capacity, such as in aerospace applications. The different results available in literature for AA2024 have been summarized in Fig. 18, both for T4 (solubilized) and for T351 (solubilized and naturally aged). Someone reported a fatigue life reduction after the application of the coating, which might originate from the loss of compressive stress in the surface and from the porous nature of the coating, offering points for stress concentration [2,3,10,86]. The worst

Fig. 17. Water Contact Angle on the surface of G16 alloy (analogous to AA2024) (a) uncoated, (b) PEO-coated, (c) PEO-coated with 2 g/L of graphene NPs. Adapted from [47].

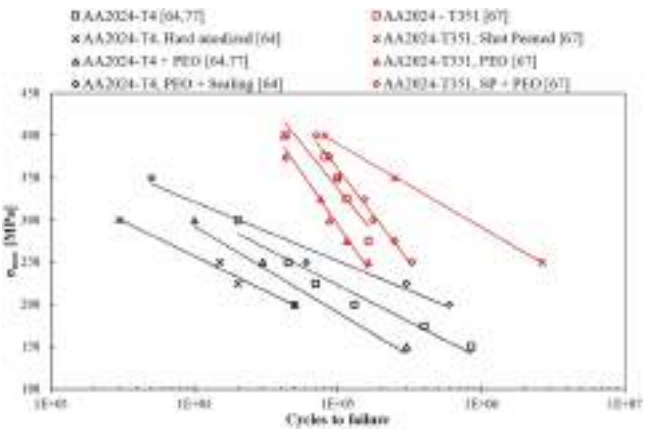

Fig. 18. Fatigue life of differently surface-finished AA2024 specimens, both with T4 and T351 thermal treatments. Data collected and adapted from [70, 73,86].

results are obtained for thick coatings [2].

However, Shreshta and Dunn reported that even though the PEO coating reduces the fatigue strength of the Al alloy, this reduction is incomparably lower than the one caused by a hard anodized coating [4]. These facts are confirmed by the results of Wang et al., which are reported in Fig. 18. Furthermore, PEO coatings are efficient in protecting the substrate from fatigue corrosion, which is often an issue in aerospace applications [4]. Different solutions have been proposed for this issue: Asquith et al. removed this impairment by shot-peening of the surface before coating [73], while Wang et al. obtained, by sealing cracks and porosities with epoxy resin, a large increase in fatigue life of alloy 2024 (Fig. 18) [70]. In the latter case, the final resistance was even larger than the one of the bare specimens, since several points for stress concentration and crack nucleation have been removed by sealing the flaws [70]. In both cases, it can be seen in Fig. 18 that the final fatigue resistance is larger than the one of the bare alloy, thus it can be concluded that, if provided with a proper pre- or post-treatment, a PEO coating can have a beneficial effect on the fatigue strength of AA2024.

There are only a few results instead of PEO coated AA2024 specimens tensile testing. Terleeva et al. reported a slight reduction in the yielding stress and the failure stress, with no significant variations in the strain at failure [86]. However, this was measured on 2 mm thick specimens, thus the effect of the ceramic layer might be lower on thicker specimens.

12. Corrosion resistance of PEO coated AA2024

The effect of a PEO coating upon the corrosion of aluminum alloy AA2024 is twofold, both slowing down the cathodic process by reducing the oxygen availability at the substrate-electrolyte interface and inducing a passive anodic behavior to the coated metal [88]. The effect on the cathodic process becomes much more evident if a pore sealing treatment is applied [28].

By considering the typical aeronautical applications of AA2024, it is evident that a PEO coating should offer good resistance against the penetration of the chloride ions. Indeed, once the PEO coated components are exposed to an aggressive environment (seawater, for instance), corrosion starts from the coating defects, where the electrolyte can reach easily the metal surface. There, the chlorides cause the rupture of the weak passive film typical of the aluminum 2xxx series, causing the initiation of a pit [28,72,88]. The corrosion evolution of PEO-coated AA2024 can be thus divided into three main stages:

- The penetration of the corrosion medium into the defects of the inner coating layer, until reaching the metallic substrate,

- The pitting corrosion of the substrate under the coating, initiating when the corrosive electrolyte arrives at the substrate-coating interface,
- The diffusion-controlled corrosion: the coating gets more damaged, exposing a larger substrate extent to the electrolyte and creating larger pores through which corrosion products can travel [28,72,88].

There is an evident effect of the quality of the PEO coating on the first step of the process: finer pores would delay the penetration of the corrosive medium [72], thus, closing them with a sealing post-treatment would noticeably increase this time lapse [88].

Localized corrosion occurs due to the galvanic coupling of the Al matrix with the Cu-rich intermetallic particles, acting as cathodes. Mg-rich phases, instead, act as anodes and undergo dealloying. Mg and Al are depleted, leaving Cu-rich remnants that may act as cathodes, thus enhancing galvanic coupling [28]. Corrosion initiation takes place at the bottom of the coating pores, where the substrate is more exposed. Then, during penetration the enlargement of existing pores and the creation of new ones is observed, thus favoring the arrival of corrosive species to the metallic surface and the removal of corrosion products from it [67]. For AA2024, corrosion products mainly consist of aluminum oxide and hydroxide and, even though in much smaller amounts, magnesium hydroxide [28]. After a certain time, the transported corrosion products accumulate on the coating surface, as shown in Fig. 19a [88]. Crack nucleation and growth on the coating surface has been observed too during corrosion (Fig. 19b). Different mechanisms have been proposed for their origin [88].

In atmospheric exposure, the corrosion products formed remain in the coating pores and deposit onto the corrosion active sites. This leads to a slight increase in the free corrosion potential of the surface and a slight decrease in the corrosion current, even though the pitting potential decreases, indicating a higher susceptibility to localized corrosion [28]. Mass loss measurements outline the effectiveness of PEO coatings against atmospheric corrosion, even though further protection can be obtained by pore sealing [28].

In water immersion, instead, the corrosion products formed inside the pores are washed away easily due to their solubility in water, thus making even more necessary the pore sealing treatment [28]. Corrosion current increases and polarization resistance decreases, contrary to the atmospheric case, since corrosion products cannot precipitate at the bottom of the flaws. All these phenomena are less evident on sealed specimens [28]. Mass loss measurements indicate a 12-time slower corrosion on coated specimens and a 200-time slower corrosion on PEO coated and sealed ones [28].

Since PEO-coated AA2024 components are frequently subjected to mechanical loading during service, their interactions with corrosion must be accounted too. In the literature, there are only some contributions about corrosion fatigue and wear corrosion.

As already explained in the related section, PEO coatings have a negative effect on the fatigue resistance of the AA2024 alloy. However, their presence, despite reducing the fatigue life of the component, can make it less susceptible to corrosion fatigue [4]. Fig. 20 shows that while pre-corroded Al specimens experience a 6 times shorter fatigue life, pre-corroded PEO-coated specimens have almost the same fatigue life as a PEO-coated specimen. This means that, when the coating is present, corrosion does not affect the fatigue life [4].

For wear-corrosion, instead, Ding et al. have reported that there is a negative synergy between corrosion and fretting wear mode, leading to a faster mass loss both in seawater and in rainwater [87]. However, as could be expected, wear losses are larger in seawater than in rainwater, because of the more aggressive environment [87].

Corrosion testing of PEO coatings is mainly done by exposure, accelerated or on field, or by electrochemical methods such as the measurement of the free corrosion potential, the potentiodynamic polarization test (PdP), or the electrochemical impedance spectroscopy (EIS).

Most of the accelerated exposure tests are carried out by immersion in solutions simulating seawater (usually, artificial seawater or 3.5% NaCl) or by using the neutral salt spray test according to the ASTM B117 standard [33,68]. The evolution of corrosion during exposure tests is monitored by looking at the surface appearance or by repeating, at fixed intervals, the measurements taken also before the exposure started (usually, PdP, EIS or microscopy) [28,33,68]. Alternatively, during immersion tests it is possible to record continuously parameters such as the free corrosion potential and the corrosion current, even if this practice is less diffused [65].

Electrochemical measurements are usually run in a 3.5 wt% NaCl solution [88], even though it is not uncommon to find alternative electrolytes, such as 0.5 M NaCl [84] or 3 wt% NaCl [28]. Potentiodynamic polarization (PdP) is one of the most used methods, even though it is destructive since some localized corrosion spots often appear at the end of the test [28]. The usual PdP curves of bare and PEO-coated AA2024 are shown in Fig. 21a [21,28]. Common values for the free corrosion potential (E_{corr}) of non-coated AA2024 are around -0.6 / -0.7 V SSC [21], even though lower values have been seldom reported [28,88]. In all cases, however, a well-formed PEO coating would shift the potential to higher values [21,88].

A PEO coating acts both on the cathodic branch and on the anodic branch of the polarization curve. The limit current density decreases by one or two orders of magnitude in the presence of a well-formed coating [21,28,63], while the anodic behavior of the coated surface turns from active into passive if the coating has low porosity and is thick enough [88]. This last aspect can be measured in terms of anodic Tafel slope (β_a) [63]. The presence of a sealing, as in Fig. 21b, referred to PTFE sealing, would further increase the free corrosion potential, decrease the corrosion current density and enhance the passive character of the anodic polarization branch [28].

EIS testing of PEO-coated alloys could provide information about the

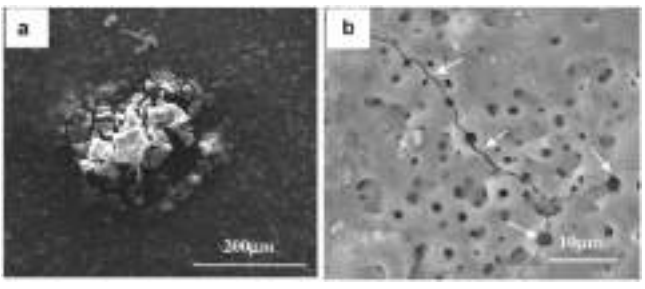

Fig. 19. (a) Corrosion product accumulation and (b) crack initiation on the surface of a PEO-coated AA2024 specimen during simulated marine exposure. Adapted from [88].

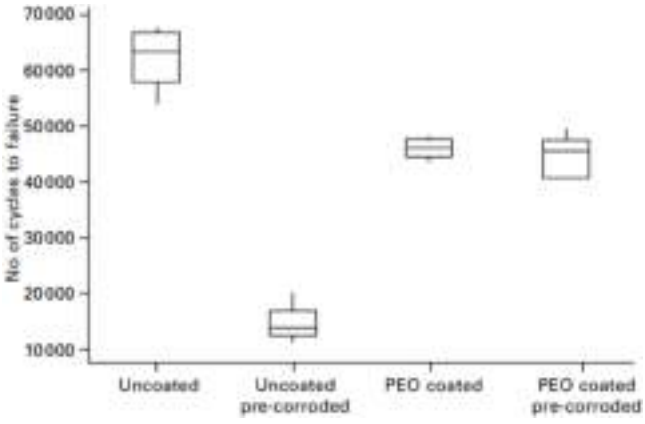

Fig. 20. Effect of a PEO coating on the corrosion-fatigue life of an Al alloy belonging to the AA2000 series. Adapted from [4].

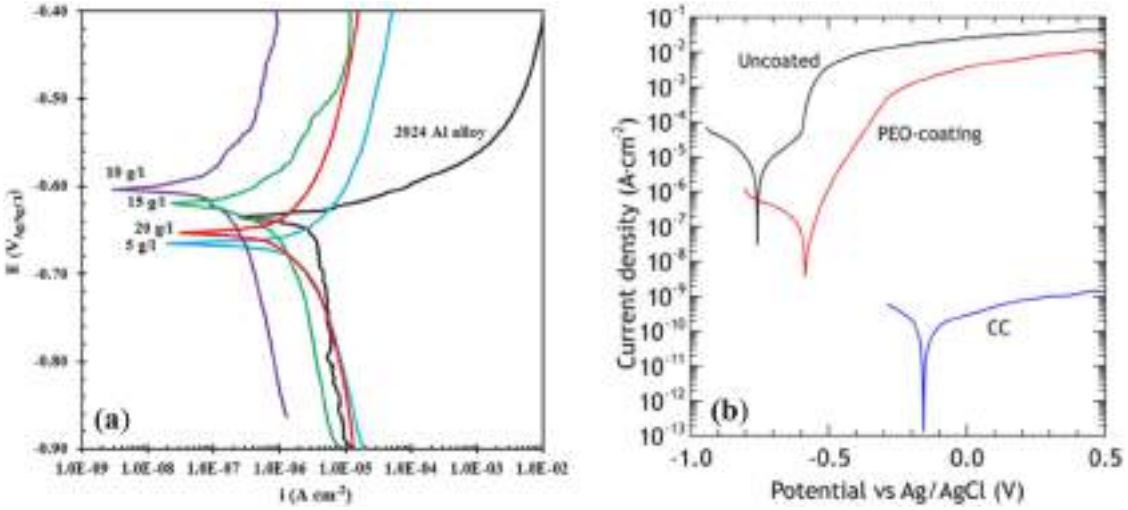

Fig. 21. Polarization curves of (a) bare and PEO-coated AA2024 specimens with different concentrations of disodium phosphate in the electrolyte, measured in 3.5% NaCl and (b) bare, PEO-coated and PEO-coated and PTFE sealed AA2024 specimens, obtained in 3% NaCl. Adapted from (a) [21], (b) [28].

structure of the coating, its porosity, its polarization resistance and the presence of defects and ongoing corrosion phenomena under it. Furthermore, the impedance behavior of PEO coatings evolves with time during exposure, giving an important insight into the ongoing chemical and physical processes [89].

As a general rule, EIS results of PEO coated aluminum display a double capacitive loop in the Nyquist plot (Z_{re} vs $-Z_{im}$), where the high frequency one represents the outer porous coating layer while the lower frequency one is related to the inner compact coating layer [89]. The most accounted equivalent circuit (EC) for modeling this behavior is the one in Fig. 22a [5,72,76,89]. Some authors report a slightly different equivalent circuit for describing the abovementioned scenarios, in which the RC parallels referring to the coating layers are not inserted one into the other but placed in series, as in Fig. 22b. Despite the results and the interpretation of these two models are quite similar [5,88], the one in Fig. 22b is more suitable for the earliest stages of corrosion. Then, as the corrosive medium starts penetrating, the previous circuits appear to be more suitable [5,88].

Other models are required instead for fitting the EIS data obtained during a prolonged exposure since the coating evolves during it. After a certain time, a third capacitive loop should appear, representative of the charge transfer at the substrate/electrolyte interface, at the bottom of the coating pores [40,89]. This means that corrosion has started, and the best interpretation is offered by the EC in Fig. 22c [76,89]. Zhang et al. proposed instead slightly different ways of incorporating the charge transfer contribution into the equivalent circuit, shown in Fig. 22d-e [39].

At longer exposure times, if the inner coating layer gets severely damaged and defective, it can be no more distinguished from the porous layer, and their half-cycles collapse into one [72,88,89]. Thus, both the intact and the damaged coating are represented by the same EC, but with a different interpretation of the elements (Fig. 22a), and distinguishing between them is not always easy. Discrimination might be done based on the values of the capacitance: the double layer capacitance (C_{dl}),

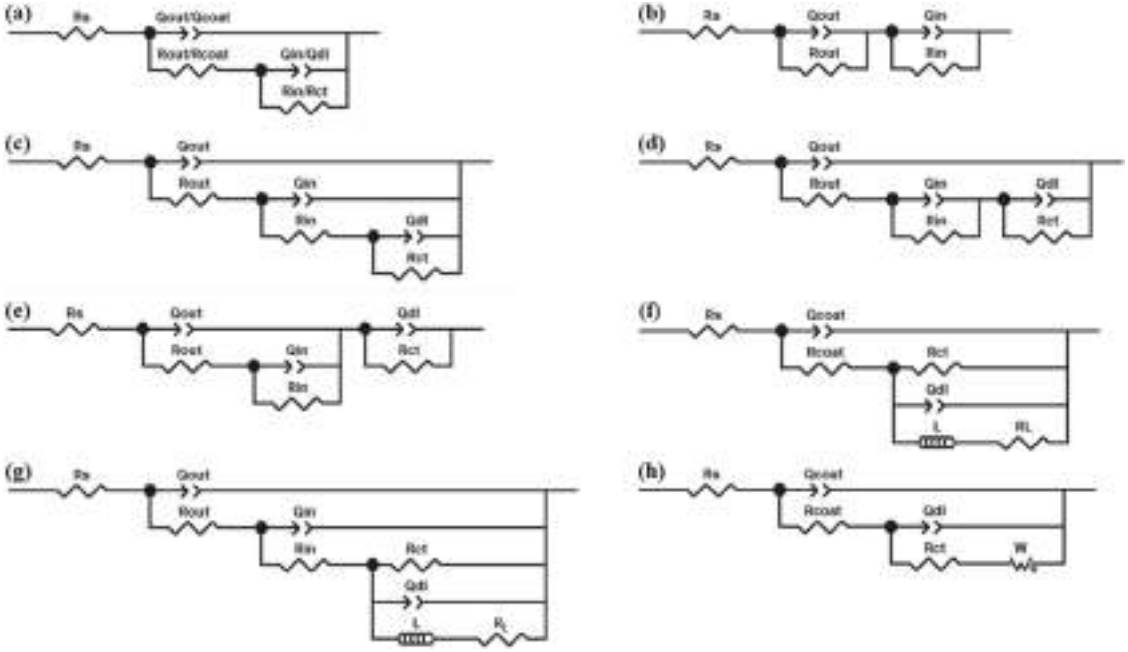

Fig. 22. Examples of equivalent circuits commonly used for EIS results interpretation of PEO coatings on aluminum. Collected and adapted from [39,76,88,89].

observed in the wetting of metallic surfaces, is usually in the μF range, while the PEO coating capacitances are usually lower (10^{-7} – 10^{-9} F) [89].

Finally, in case of extreme coating damage, the EC might be reduced to a single RC couple representing charge transfer at the substrate-electrolyte interface [67].

The diameter of every capacitive loop represents a polarization resistance value. Each of them can be associated with the corresponding coating layer, thus understanding the contribution of each layer to the overall polarization resistance. With AA2024, as immersion time increases, both the outer layer and the barrier layer R_P might increase, this, however, would represent the accumulation of non-adherent corrosion products in the pores rather than an increase in protectiveness [72,88,89].

In some cases, especially during the earliest stages of immersion, pitting corrosion could be observed under the PEO coating. In such cases, an inductor element L should be introduced, often together with a resistance R_L (localized corrosion resistance). There might be different ways of introducing them in the EC, as represented in Fig. 22f-g. This peculiar behavior, originating a loop with positive imaginary part in the Nyquist plane, could be explained as a relaxation of the adsorbed species in the corrosion pits [89].

For almost all the PEO coatings, better fit results are obtained by changing the capacitive elements with a constant phase element (CPE), representing a capacitance with non-ideal behavior. Its characteristic equation contains two parameters, a capacitance (Q) and an exponent (p). The latter ranges from 0 to 1 and, the closer it is to 1, the closer the CPE to an ideal capacitor and the higher the phase shift at high frequencies on the Bode plot [5,89]. A deviation of the parameter p from 1 indicates a higher coating roughness and defectiveness, thus an easier penetration of the corrosive media [89]. During immersion, capacitance values tend to increase as coating layers develop new pores and get more defective [72,88,89].

The corrosion processes can involve sometimes important diffusion phenomena, which are shown as straight lines with a 45° slope at low frequencies and can be modeled by introducing in the EC the Warburg impedance element, representative of diffusion with semi-infinite boundaries. The diffusion processes, if present, would appear only at small frequencies because at high ones the chemical species have no time enough to move in a significant way [89]. Diffusion-controlled processes might occur in PEO coatings corrosion too, but never with an ideal behavior: in this case, diffusion can occur with absorbing boundaries, modeled by a Warburg-short circuit element, or with reflective boundaries, modeled by a Warburg-open circuit element. Their corresponding Nyquist characteristics are shown in Fig. 23 [89]. The transport of corrosive species through pores sealed with resistance, such as an oxide film, at one end usually shows up as Warburg shorts. Similar diffusion processes, but with an impermeable barrier at the end of the pore, can be modeled usually by a Nyquist-open circuit element [89].

All the Warburg elements contain a Warburg resistance term which decreases as the electrolyte penetration pathways through the coating become more numerous [89]. However, also the increase of the Warburg impedance value has been observed, motivated by the clogging of the pores with the transported corrosion products [88]. A possible way of inserting a Warburg element in the EC of a PEO coating on AA2024 is given in Fig. 22h [88].

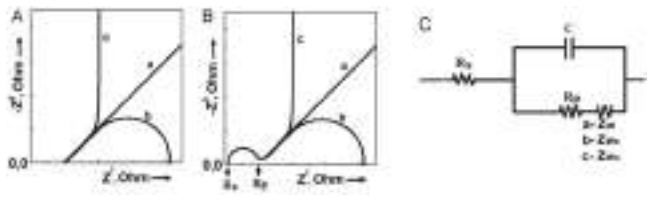

Fig. 23. (a) Zre – Zim behavior of a Warburg element, (b) Zre – Zim behavior of a Warburg impedance into the RC parallel shown in (c). In (a) and (b), a, b, and c labels correspond respectively to a Warburg-ideal, a Warburg-short, and a Warburg-open behavior. Adapted from [89].

Sealed PEO coatings usually present the same EIS features as unsealed ones but with different values of resistance and capacitance. Thus, they are often interpreted with the same abovementioned ECs, but obtain higher resistance values [28,68] and a phase angle increase at low frequency, which can be very large if the sealed surface is hydrophobic [28,47].

The electrochemical testing results show a correlation with the PEO coating thickness. Fig. 24 shows that thicker coatings can provide a more effective protection from corrosion, with lower values of corrosion current density (i_{corr}) and larger impedance at low frequencies in EIS. However, there are other parameters influencing the protectiveness of a coating, such as its porosity or its composition, which cannot be neglected.

13. PEO coatings for surface functionalization

The PEO process can be regarded also as an opportunity for producing a functional coating, namely a coating endowing the component surface with a peculiar ability. There are some examples in which by means of a peculiar PEO process the AA2024 surface has been featured with photochemical or corrosion inhibition activity or has been made hydrophobic or self-lubricating.

Photocatalytic activity has been observed by Mojsilovic et al. on the surface of AA2024 specimens after the PEO coating into an electrolyte containing potassium titanium oxide oxalate and ZnAl layered double hydroxides (LDH) [49]. The resulting coating was enriched with titanium oxides, mixed oxides of titanium and potassium and zinc-aluminum oxides, and showed a maximum photocatalytic activity (namely, the ability to accelerate a photo-induced reaction) of 52%, even in the visible range of the electromagnetic spectrum [49].

The surface wettability of the PEO coating of D16T alloy (equivalent to AA2024) has been modified by introducing different amounts of graphene nanoparticles in the electrolyte. Normally, PEO coatings are hydrophilic, often even more than the bare substrate. As visible from Fig. 17, by introducing graphene, the coating behavior can be changed into hydrophobic [47]. PEO coatings of Al can be endowed with superhydrophobicity too, for instance by pore sealing with fluorinated compounds [71]. However, the durability of the obtained coatings is quite short [71].

There are, then, some examples of PEO coatings endowed with corrosion inhibiting features by loading them with proper additives, both during the coating process or during the post-treatment. Del Olmo et al. showed the possibility of loading Ce^{3+} and WO_4^{2-} even in very thin PEO coatings (≈ 5 μm) of AA2024, greatly enhancing its corrosion resistance, with a polarization resistance value increased by two orders of magnitude [33,69]. However, due to the nature of the inserted species and the low thickness of the coating, exposure to an aggressive environment such as seawater quickly reduces corrosion resistance [33]. Akbarzadeh et al., instead, induced a self-healing ability in the PEO coating of alloy AA2024 by alternating onto it layers of corrosion inhibitors and of a sol-gel organic sealing [67].

Finally, also the friction coefficient of the PEO coating surface might be tuned by properly modifying the PEO process, as reported in paragraph 11.

There are then other examples of PEO coatings for surface functionalization regarding pure aluminum as substrate material: for instance, Santos et al. succeeded in incorporating silver obtaining a significant antibacterial action. The *Bacillus Subtilis* bacteria, used in this case study, colonized more difficultly the PEO-coated specimens produced in the presence of Ag^+ cations and sodium silicates [50].

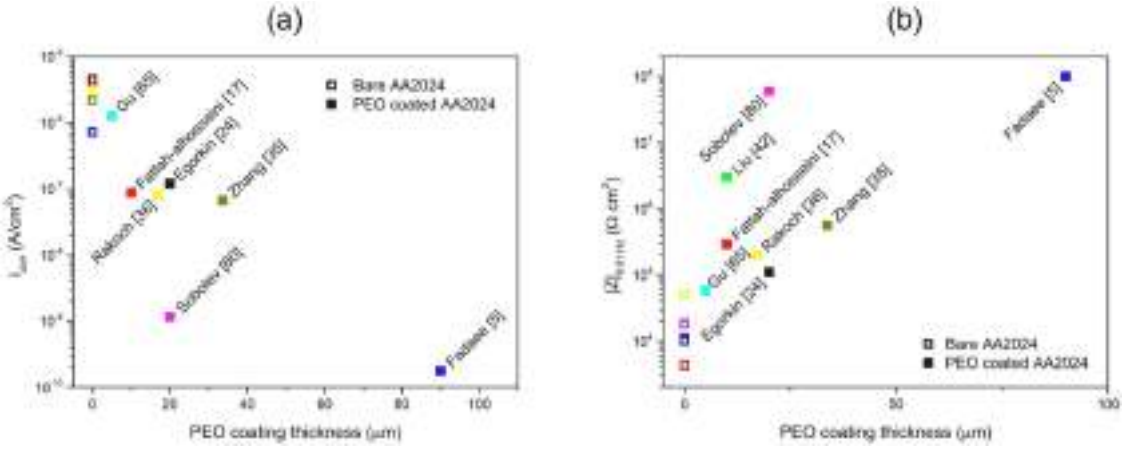

Fig. 24. Correlation between PEO coating thickness and (a) corrosion current density (b) impedance modulus at low frequencies obtained from different works.

14. Upscaling PEO for industrial application

Despite the great research effort behind PEO coating of aluminum alloys, some issues still must be addressed to make it suitable for industrial production. Nowadays, the main limitations are the homogeneity of the coating over large workpieces, the consumption of the electrolyte constituents during coating formation, the large heat development in the electrolyte and the large energy consumption of the process when applied to large surfaces. The first one has been already addressed in paragraph 9.6. Del Olmo et al., instead, have tried facing the latter issue by dramatically reducing the treatment times, proposing the so-called "flash-PEO" in which a thin coating is produced on AA2024 [33]. However, this poses the problem of recovering the corrosion protection lost with the lost thickness, which can be only partially solved by using corrosion inhibitors [33].

A faster heat removal from the anodizing bath can be achieved by acting in different ways. Sobolev et al. increased the thermal conductivity of the electrolyte for AA2024 PEO by using low-melting molten salts (mainly $NaNO_3$) instead of the usual aqueous solution, which allows a faster heat removal but raises the process temperature from room temperature to 280°C [90]. Ropyak et al. instead optimized the process parameters for PEO coating alloy AA2024 in a flowing silicate-alkaline electrolyte. They reported maximized tribological properties with a fluid velocity of 104 cm/s [91].

Another obstacle that should be faced with the upscale of PEO coating is the treatment of huge workpieces. In this case, all the issues of coating homogeneity, energy and electrolyte consumption and heat development arise together. Spraying electrolyte micro-arc oxidation (SMAO) has been proposed as a solution for the treatment of large surfaces [17]. In this process, a pump is embedded within a movable cathode, such that the electrolyte is sprayed locally on the surface interested by the treatment. Then, the spraying cathode is moved around the surface to cover the whole workpiece extension with the coating [17]. SMAO is slower than conventional PEO but allows for electrolyte saving and on-field coating repair too [17].

Another way of decreasing the costs for electrolyte consumption in PEO upscaling could be the use of tap water as a base for the solution instead of distilled water. This has proved to be somehow effective, even though tap water introduces impurities in the bath, in an amount strongly dependent on the location of the anodizing plant [36]. The effect of impurities from the use of tap water has been already addressed in paragraph 5.1.

Despite these contributions and the birth of the first companies specialized in industrial PEO treatments, PEO remains a promising technique, and deeper work is still required to optimize this process, making it suitable for large-scale applications.

15. Conclusion

Plasma Electrolytic Oxidation (PEO) is a promising technique for coating aluminum alloy AA2024. Indeed, PEO coatings can offer this alloy large improvements in corrosion resistance, surface hardness, wear resistance and thermal insulation. Because of these features, PEO-coated AA2024 objects are finding a growing use in the fields of aerospace (launch vessels, low temperature components) [4] and technical and scientific equipment (mainly quickly moving parts requiring surface hardness and durability, such as turbo pumps) [1]. Still in this last field, PEO-coated aluminum has been used in optical devices for light absorption [1]. There are examples of PEO-coated AA2024 in the field of automobile, also as a substrate for improving adhesion of painted layers [2]. Furthermore, PEO is a quite fast treatment involving non-toxic and non-harmful chemicals. However, despite the large experimental effort of the last years, it is still necessary to achieve a deeper comprehension of the phenomena ongoing inside the plasma during the growth of the coating. Indeed, the role and effects of various control parameters remain unclear, and their selection is largely empirical, even in commercial settings. Moreover, additional research is required to scale up the PEO process, making it suitable for coating large surfaces or large batches of workpieces. This review highlights the key aspects in which research should focus to address these limitations.

CRediT authorship contribution statement

Matteo Gamba: Writing – original draft, Visualization, Investigation. **Andrea Cristoforetti:** Writing – review & editing, Visualization. **Michele Fedel:** Writing – review & editing, Project administration. **Federica Ceriani:** Writing – review & editing. **Marco Ormellese:** Supervision. **Andrea Brenna:** Writing – review & editing, Supervision, Project administration.

Declaration of competing interest

The authors declare the following financial interests/personal relationships which may be considered as potential competing interests:

Andrea Brenna reports financial support was provided by Government of Italy. If there are other authors, they declare that they have no known competing financial interests or personal relationships that could have appeared to influence the work reported in this paper.

Acknowledgements

The authors acknowledge funding by European Union – Next Generation Eu, PNRR - Missione 4 "Istruzione E Ricerca" - Componente C2 Investimento 1.1 "Fondo per il programma nazionale di ricerca e

progetti di rilevante interesse nazionale (PRIN)" D.D. N. 104/2022 "Bando Prin 2022". PE11 Engineering of Metals and Alloys.

Data availability

No data was used for the research described in the article.

References

[1] F. Simchen, M. Sieber, A. Kopp, T. Lampke, Introduction to plasma electrolytic oxidation-an overview of the process and applications, Coatings 10 (7) (2020), https://doi.org/10.3390/coatings10070628.

[2] S. Sikdar, P.V. Menezes, R. Maccione, T. Jacob, P.L. Menezes, Plasma electrolytic oxidation (PEO) process — processing, properties, and applications, Nanomaterials 11 (6) (2021), https://doi.org/10.3390/nano11061375.

[3] T.W. Clyne, S.C. Troughton, A Review of Recent Work on Discharge Characteristics During Plasma Electrolytic Oxidation of Various Metals, Taylor and Francis Ltd, 2019, https://doi.org/10.1080/09506608.2018.1466492.

[4] S. Shrestha, B.D. Dunn, Plasma electrolytic oxidation and anodising of aluminium alloys for spacecraft applications, in: Surface Engineering of Light Alloys, 18, Woodhead Publishing Limited, 2010, pp. 603–641, ch.

[5] H. Fadaee, M. Javidi, Investigation on the corrosion behaviour and microstructure of 2024-T3 Al alloy treated via plasma electrolytic oxidation, J. Alloys Compd. 604 (2014) 36–42, https://doi.org/10.1016/j.jallcom.2014.03.127.

[6] G. Lv, et al., Characteristic of ceramic coatings on aluminum by plasma electrolytic oxidation in silicate and phosphate electrolyte, Appl. Surf. Sci. 253 (5) (2006) 2947–2952, https://doi.org/10.1016/j.apsusc.2006.06.036.

[7] A.B. Rogov, A. Yerokhin, A. Matthews, The role of cathodic current in plasma electrolytic oxidation of aluminum: phenomenological concepts of the 'soft sparking' mode, Langmuir 33 (41) (2017) 11059–11069, https://doi.org/10.1021/acs.langmuir.7b02284.

[8] P. Fernández-López, S.A. Alves, J.T. San-Jose, E. Gutierrez-Berasategui, R. Bayón, Plasma electrolytic oxidation (PEO) as a promising technology for the development of high-performance coatings on cast Al-Si alloys: a review, Coatings 14 (2) (2024), https://doi.org/10.3390/coatings14020217.

[9] R.O. Hussein, X. Nie, D.O. Northwood, Production of high quality coatings on light alloys using plasma Electrolytic Oxidation (PEO). High Performance and Optimum Design of Structures and Materials II, WIT Press, 2016, pp. 439–454, https://doi.org/10.2495/hpsm160411.

[10] Lord Famiyeh, X. Huang, Plasma electrolytic oxidation coatings on aluminum alloys: microstructures, properties, and applications, Mod. Concepts Mater. Sci. 2 (1) (2019).

[11] M.M.S. Al Bosta, K.J. Ma, H.H. Chien, The effect of MAO processing time on surface properties and low temperature infrared emissivity of ceramic coating on aluminium 6061 alloy, Infrared. Phys. Technol. 60 (2013) 323–334, https://doi.org/10.1016/j.infrared.2013.06.006.

[12] Y.J. Oh, J. Il Mun, J.H. Kim, Effects of alloying elements on microstructure and protective properties of Al2O3 coatings formed on aluminum alloy substrates by plasma electrolysis, Surf. Coat. Technol. 204 (1–2) (2009) 141–148, https://doi.org/10.1016/j.surfcoat.2009.07.002.

[13] M. Sieber, F. Simchen, R. Morgenstern, I. Scharf, T. Lampke, Plasma electrolytic oxidation of high-strength aluminium alloys—substrate effect on wear and corrosion performance, Metals 8 (5) (2018), https://doi.org/10.3390/met8050356.

[14] A.B. Rogov, V.R. Shayapov, Correlations between the optical emission spectra and microstructure of microplasma coatings on aluminum 2024 alloy, Appl. Surf. Sci. 258 (11) (2012) 4871–4876, https://doi.org/10.1016/j.apsusc.2012.01.097.

[15] K. Tillous, T. Toll-Duchanoy, E. Bauer-Grosse, L. Hericher, G. Geandier, Microstructure and phase composition of microarc oxidation surface layers formed on aluminium and its alloys 2214-T6 and 7050-T74, Surf. Coat. Technol. 203 (19) (2009) 2969–2973, https://doi.org/10.1016/j.surfcoat.2009.03.021.

[16] D. Salehi Doolabi, M. Ehteshamzadeh, S.M.M. Mirhosseini, Effect of NaOH on the structure and corrosion performance of alumina and silica PEO coatings on aluminum, J. Mater. Eng. Perform. 21 (10) (2012) 2195–2202, https://doi.org/10.1007/s11665-012-0151-1.

[17] L. Wen, Y. Wang, Y. Jin, B. Liu, Y. Zhou, D. Sun, Microarc oxidation of 2024 Al alloy using spraying polar and its influence on microstructure and corrosion behavior, Surf. Coat. Technol. 228 (2013) 92–99, https://doi.org/10.1016/j.surfcoat.2013.04.013.

[18] M. Vakili-Azghandi, A. Fattah-alhosseini, M.K. Keshavarz, Optimizing the electrolyte chemistry parameters of PEO coating on 6061 Al alloy by corrosion rate measurement: response surface methodology, Measurement 124 (2018) 252–259, https://doi.org/10.1016/j.measurement.2018.04.038.

[19] F. Ceriani, L. Casanova, M. Ormellese, Use of organic acids as additives for plasma electrolytic oxidation (PEO) of titanium, Coatings 14 (6) (2024), https://doi.org/10.3390/coatings14060703.

[20] J. Liang, Z. Peng, X. Cui, R. Li, B. Wang, Comparison of plasma electrolytic oxidation coatings on Al alloy produced in diluted and concentrated silicate electrolytes for space thermal control application, Ceram. Int. 50 (4) (2024) 6349–6357, https://doi.org/10.1016/j.ceramint.2023.11.367.

[21] A. Fattah-alhosseini, S.O. Gashti, M. Molaie, Effects of disodium phosphate concentration (Na2HPO4·2H2O) on microstructure and corrosion resistance of plasma electrolytic oxidation (PEO) coatings on 2024 Al alloy, J. Mater. Eng. Perform. 27 (2) (2018) 825–834, https://doi.org/10.1007/s11665-018-3124-1.

[22] M. Javidi, H. Fadaee, Plasma electrolytic oxidation of 2024-T3 aluminum alloy and investigation on microstructure and wear behavior, Appl. Surf. Sci. 286 (2013) 212–219, https://doi.org/10.1016/j.apsusc.2013.09.049.

[23] A.B. Rogov, V.R. Shayapov, The role of cathodic current in PEO of aluminum: influence of cationic electrolyte composition on the transient current-voltage curves and the discharges optical emission spectra, Appl. Surf. Sci. 394 (2017) 323–332, https://doi.org/10.1016/j.apsusc.2016.10.115.

[24] D.S. Tsai, C.C. Chou, Review of the soft sparking issues in plasma electrolytic oxidation, Metals 8 (2) (2018), https://doi.org/10.3390/met8020105.

[25] V.M. Posuvailo, V.V. Kulyk, Z.A. Duriagina, I.V. Koval'chuck, M.M. Student, B. D. Vasyliv, The effect of electrolyte composition on the plasma electrolyte oxidation and phase composition of oxide ceramic coatings formed on 2024 aluminium alloy, Arch. Mater. Sci. Eng. 105 (2) (2020) 49–55, https://doi.org/10.5604/01.3001.0014.5761.

[26] M. Student, H.H. Veselivska, O.S. Kalakhan, V. Hvozdetskyi, K.R. Zadorozhna, Y. Y. Sirak, Influence of the conditions of plasma-electrolytic treatment of D16T aluminum alloy on its corrosion resistance in 3% NaCl solution, Mater. Sci. 56 (4) (2021) 550–559, https://doi.org/10.1007/s11003-021-00463-z.

[27] L.M. Bilyi, V.M. Posuvailo, V.R. Ivashkiv, I.V. Kovalchuk, Corrosion properties of oxide ceramic coatings based on alloys of the Al–Cu–Mg and Al–Mg systems, Mater. Sci. 57 (2) (2021) 256–263, https://doi.org/10.1007/s11003-021-00540-3.

[28] V.S. Egorkin, et al., Atmospheric and marine corrosion of PEO and composite coatings obtained on Al-Cu-Mg aluminum alloy, Materials 13 (12) (2020), https://doi.org/10.3390/ma13122739.

[29] Q. Zhang, et al., The influence of EDTA-2Na on microstructure and corrosion resistance of PEO coating for AA1060 alloy, Int. J. Appl. Ceram. Technol. 18 (3) (2021) 928–936, https://doi.org/10.1111/ijac.13696.

[30] M.P. Kamil, M. Kaseem, Y.G. Ko, Soft plasma electrolysis with complex ions for optimizing electrochemical performance, Sci. Rep. 7 (2017), https://doi.org/10.1038/srep44458.

[31] A. Olesiński, A. Bugla, D. Babilas, A. Stolarczyk, W. Simka, M. Sowa, Corrosion performance of 6061 aluminium alloy protected by plasma electrolytic oxidation coatings modified by acrylic acid, Corros. Sci. 237 (2024), https://doi.org/10.1016/j.corsci.2024.112322.

[32] L. Casanova, F. Ceriani, M. Pedeferri, M. Ormellese, Addition of organic acids during PEO of titanium in alkaline solution, Coatings 12 (2) (2022), https://doi.org/10.3390/coatings12020143.

[33] R. del Olmo, M. Mohedano, P. Visser, E. Matykina, R. Arrabal, Flash-PEO coatings loaded with corrosion inhibitors on AA2024, Surf. Coat. Technol. 402 (2020), https://doi.org/10.1016/j.surfcoat.2020.126317.

[34] Y. Cheng, X. Shi, Y. Lv, X. Zhang, Effect of electrolyte temperature on plasma electrolytic oxidation of pure aluminum, Metals 14 (6) (2024), https://doi.org/10.3390/met14060615.

[35] X. Wu, W. Qin, Y. Guo, Z. Xie, Self-lubricative coating grown by micro-plasma oxidation on aluminum alloys in the solution of aluminate-graphite, Appl. Surf. Sci. 254 (20) (2008) 6395–6399, https://doi.org/10.1016/j.apsusc.2008.04.001.

[36] O.P. Terleeva, A.I. Slonova, A.B. Rogov, V.V. Kokovkin, I.V. Mironov, Effect of chloride and sulphate anions as minor impurities in silicate alkaline electrolyte on plasma electrolytic oxidation of aluminium alloys, Mater. Res. Express. 6 (1) (2019), https://doi.org/10.1088/2053-1591/aae3f4.

[37] S. Rahimi, B. Yarmand, A. Kolahi, Effects of process parameters on structure and corrosion behavior of PEO coated A356 alloy, Surf. Topogr. 8 (4) (2020), https://doi.org/10.1088/2051-672X/abc736.

[38] Y.L. Cheng, H.J. Xie, J.H. Cao, Y.L. Cheng, Effect of NaOH on plasma electrolytic oxidation of A356 aluminium alloy in moderately concentrated aluminate electrolyte, Trans. Nonferrous Metals Soc. China 31 (12) (2021) 3677–3690, https://doi.org/10.1016/S1003-6326(21)65756-4.

[39] D. Zhang, Y. Ran, X. Chen, J. Xia, L. Cai, W. Ping, Role of rare-earth Y addition on formation and anticorrosion properties of MAO coating on 2024 aviation aluminum alloy, Int. J. Appl. Ceram. Technol. 20 (1) (2023) 451–464, https://doi.org/10.1111/ijac.14246.

[40] A.G. Rakoch, et al., Role of cobalt additive on formation and anticorrosion properties of PEO coatings on AA2024 alloy in alkali-silicate electrolyte, Surf. Coat. Technol. 433 (2022), https://doi.org/10.1016/j.surfcoat.2021.128075.

[41] G.A. Mengesha, J.P. Chu, B.S. Lou, J.W. Lee, Effects of processing parameters on the corrosion performance of plasma electrolytic oxidation grown oxide on commercially pure aluminum, Metals 10 (3) (2020), https://doi.org/10.3390/met10030394.

[42] Y. Gao, et al., Effect of h-BN nanoparticles incorporation on the anti-corrosion and anti-wear properties of micro-arc oxidation coatings on 2024 aluminum alloy, Ceram. Int. 49 (23) (2023) 37475–37485, https://doi.org/10.1016/j.ceramint.2023.09.074.

[43] K. Xi, et al., Improved corrosion and wear resistance of micro-arc oxidation coatings on the 2024 aluminum alloy by incorporation of quasi-two-dimensional sericite microplates, Appl. Surf. Sci. 585 (2022), https://doi.org/10.1016/j.apsusc.2022.152693.

[44] K. Babaei, A. Fattah-alhosseini, M. Molaei, The effects of carbon-based additives on corrosion and wear properties of plasma electrolytic oxidation (PEO) coatings applied on aluminum and its alloys: a review, Surf. Interfaces 21 (2020), https://doi.org/10.1016/j.surfin.2020.100677.

[45] Z. Li, S. Di, The microstructure and wear resistance of microarc oxidation composite coatings containing nano-hexagonal boron nitride (HBN) particles, J. Mater. Eng. Perform. 26 (4) (2017) 1551–1561, https://doi.org/10.1007/s11665-017-2582-1.

[46] O.P. Terleeva, A.I. Slonova, A.B. Rogov, A. Matthews, A. Yerokhin, Wear resistant coatings with a high friction coefficient produced by plasma electrolytic oxidation of al alloys in electrolytes with basalt mineral powder additions, Materials 12 (7) (2019), https://doi.org/10.3390/ma12172738.
[47] W. Liu, et al., Effect of graphene on the microstructure and corrosion resistance of PEO coating formed on D16T aluminum alloy, Int. J. Appl. Ceram. Technol. 19 (5) (2022) 2583–2597, https://doi.org/10.1111/ijac.14108.
[48] M. Vakili-Azghandi, A. Fattah-alhosseini, Effects of duty cycle, current frequency, and current density on corrosion behavior of the plasma electrolytic oxidation coatings on 6061 Al alloy in artificial seawater, Metall. Mater. Trans. a Phys. Metall. Mater. Sci. 48 (10) (2017) 4681–4692, https://doi.org/10.1007/s11661-017-4205-8.
[49] K. Mojsilović, M. Serdechnova, C. Blawert, M.L. Zheludkevich, S. Stojadinović, R. Vasilić, In-situ incorporation of LDH particles during PEO processing of aluminium alloy AA2024, Appl. Surf. Sci. 654 (2024), https://doi.org/10.1016/j.apsusc.2024.159450.
[50] J.S. Santos, et al., One-step synthesis of antibacterial coatings by plasma electrolytic oxidation of aluminum, Adv. Eng. Mater. 21 (8) (2019), https://doi.org/10.1002/adem.201900119.
[51] R. Liu, et al., Discharge behaviors during plasma electrolytic oxidation on aluminum alloy, Mater. Chem. Phys. 148 (1–2) (2014) 284–292, https://doi.org/10.1016/j.matchemphys.2014.07.045.
[52] S.P. Sah, E. Tsuji, Y. Aoki, H. Habazaki, Cathodic pulse breakdown of anodic films on aluminium in alkaline silicate electrolyte - understanding the role of cathodic half-cycle in AC plasma electrolytic oxidation, Corros. Sci. 55 (2012) 90–96, https://doi.org/10.1016/j.corsci.2011.10.007.
[53] S. Xin, L. Song, R. Zhao, X. Hu, Influence of cathodic current on composition, structure and properties of Al2O3 coatings on aluminum alloy prepared by micro-arc oxidation process, Thin. Solid. Films. 515 (1) (2006) 326–332, https://doi.org/10.1016/j.tsf.2005.12.087.
[54] F. Ceriani, L. Casanova, L. Massimini, A. Brenna, M. Ormellese, TiO2 microparticles incorporation in coatings produced by plasma electrolytic oxidation (PEO) on titanium, Coatings 13 (10) (2023), https://doi.org/10.3390/coatings13101718.
[55] A.B. Rogov, A. Yerokhin, A. Matthews, The role of cathodic current in plasma electrolytic oxidation of aluminium: current density 'scanning waves' on complex-shape substrates, J. Phys. D. Appl. Phys. 51 (40) (2018), https://doi.org/10.1088/1361-6463/aad979.
[56] K. Du, X. Guo, Q. Guo, F. Wang, Y. Tian, A monolayer PEO coating on 2024 Al alloy by transient self-feedback control mode, Mater. Lett. 91 (2013) 45–49, https://doi.org/10.1016/j.matlet.2012.09.055.
[57] A.L. Yerokhin, et al., Oxide ceramic coatings on aluminium alloys produced by a pulsed bipolar plasma electrolytic oxidation process, Surf. Coat. Technol. 199 (2-3) (2005) 150–157, https://doi.org/10.1016/j.surfcoat.2004.10.147.
[58] L. Zhu, W. Zhang, H. Liu, L. Liu, F. Wang, Z. Qiao, Single dense layer of PEO coating on aluminum fabricated by 'chain-like' discharges, Materials 15 (13) (2022), https://doi.org/10.3390/ma15134635.
[59] L.Y. An, Y. Ma, X.X. Yan, S. Wang, Z. ying Wang, Effects of electrical parameters and their interactions on plasma electrolytic oxidation coatings on aluminum substrates, Trans. Nonferrous Metals Soc. China 30 (4) (2020) 883–895, https://doi.org/10.1016/S1003-6326(20)65262-1.
[60] Z. Li, S. Di, Preparation and properties of micro-arc oxidation self-lubricating composite coatings containing paraffin, J. Alloys. Compd. 719 (2017) 1–14, https://doi.org/10.1016/j.jallcom.2017.05.138.
[61] A.B. Rogov, A. Nemcova, T. Hashimoto, A. Matthews, A. Yerokhin, Analysis of electrical response, gas evolution and coating morphology during transition to soft sparking PEO of Al, Surf. Coat. Technol. 442 (2022), https://doi.org/10.1016/j.surfcoat.2022.128142.
[62] V. Ntomprougkidis, J. Martin, A. Nominé, G. Henrion, Sequential run of the PEO process with various pulsed bipolar current waveforms, Surf. Coat. Technol. 374 (2019) 713–724, https://doi.org/10.1016/j.surfcoat.2019.06.057.
[63] H. Yan, et al., Effects of micro-arc oxidation process parameters on micro-structure and properties of Al2O3 coatings prepared on sintered 2024 aluminum alloy, J. Mater. Eng. Perform. 33 (4) (2024) 1862–1873, https://doi.org/10.1007/s11665-023-08093-z.
[64] C. Lu, et al., Influence of surface microstructure on tribological properties of PEO-PTFE coating formed on aluminum alloy, Surf. Coat. Technol. 364 (2019) 127–134, https://doi.org/10.1016/j.surfcoat.2019.02.064.
[65] S.V. Oleynik, V.S. Rudnev, Y.A. Kuzenkov, T.P. Jarovaja, L.F. Trubetskaja, P. M. Nedozorov, Protective properties of PEO coatings modified by corrosion inhibitors on aluminum alloys, Int. J. Corros. Scale Inhibit. 6 (2) (2017) 91–111, https://doi.org/10.17675/2305-6894-2017-6-2-1.
[66] C. Lu, J. Ding, P. Shi, J. Jia, E. Xie, Y. Sun, Effects of texture density on the tribological properties of plasma electrolytic oxidation/polytetrafluoroethylene coatings formed on aluminum alloys, Macromol. Mater. Eng. 307 (2) (2022), https://doi.org/10.1002/mame.202100678.
[67] S. Akbarzadeh, L.B. Coelho, L. Dangreau, A. Lanzutti, L. Fedrizzi, M.G. Olivier, Self-healing plasma electrolytic oxidation (PEO) coating developed by an assembly of corrosion inhibitive layer and sol-gel sealing on AA2024, Corros. Sci. 222 (2023), https://doi.org/10.1016/j.corsci.2023.111424.
[68] G. Liu, X. Lu, X. Zhang, T. Zhang, F. Wang, Improvement of corrosion resistance of PEO coatings on Al alloy by formation of ZnAl layered double hydroxide, Surf. Coat. Technol. 441 (2022), https://doi.org/10.1016/j.surfcoat.2022.128528.
[69] R. del Olmo, et al., Hybrid PEO/sol-gel coatings loaded with Ce for corrosion protection of AA2024-T3, Prog. Org. Coat. 182 (2023), https://doi.org/10.1016/j.porgcoat.2023.107667.
[70] X.S. Wang, X.W. Guo, X.D. Li, D.Y. Ge, Improvement on the fatigue performance of 2024-T4 alloy by synergistic coating technology, Materials 7 (5) (2014) 3533–3546, https://doi.org/10.3390/ma7053533.
[71] Q. Zhu, X. Du, Y. Liu, X. Fang, D. Chen, Z. Zhang, Preparation and applications of superhydrophobic coatings on aluminum alloy surface for anti-corrosion and anti-fouling: a mini review, Coatings 13 (11) (2023), https://doi.org/10.3390/coatings13111881.
[72] Y. Gu, H. Ma, W. Yue, B. Tian, L. Chen, D. Mao, Microstructure and corrosion model of MAO coating on nano grained AA2024 pretreated by ultrasonic cold forging technology, J. Alloys. Compd. 681 (2016) 120–127, https://doi.org/10.1016/j.jallcom.2016.03.196.
[73] D.T. Asquith, A.L. Yerokhin, J.R. Yates, A. Matthews, Effect of combined shot-peening and PEO treatment on fatigue life of 2024 Al alloy, Thin. Solid. Films. 515 (3) (2006) 1187–1191, https://doi.org/10.1016/j.tsf.2006.07.123.
[74] L. Wen, Y. Wang, Y. Zhou, L. Guo, J.H. Ouyang, Microstructure and corrosion resistance of modified 2024 Al alloy using surface mechanical attrition treatment combined with microarc oxidation process, Corros. Sci. 53 (1) (2011) 473–480, https://doi.org/10.1016/j.corsci.2010.09.061.
[75] L. Wen, Y. Wang, Y. Jin, D. Sun, Fabrication and characterization of multiscale graded SMAT-MAO composite coating formed on the surface of 2024 Al alloy. Journal of Physics: Conference Series, Institute of Physics Publishing, 2013, https://doi.org/10.1088/1742-6596/419/1/012031.
[76] M.A. Iqbal, E. Matykina, R. Arrabal, M. Mohedano, Role of anodic precursor layer thickness on PEO coatings: energy consumption and long-term corrosion performance, Surf. Coat. Technol. 476 (2024), https://doi.org/10.1016/j.surfcoat.2023.130186.
[77] C. Fan, et al., Adhesion strength and anti-corrosion performance of ceramic coating on laser-textured aluminum alloy, Coatings 13 (12) (2023), https://doi.org/10.3390/coatings13122098.
[78] B. Jaleh, A. Nasri, R. Chaharmahali, M. Kaseem, A. Fattah-alhosseini, Exploring wear, corrosion, and microstructure in PEO coatings via laser surface treatments on aluminum substrates, Opt. Laser. Technol. 181 (2025), https://doi.org/10.1016/j.optlastec.2024.111958.
[79] R.O. Hussein, X. Nie, D.O. Northwood, A. Yerokhin, A. Matthews, Spectroscopic study of electrolytic plasma and discharging behaviour during the plasma electrolytic oxidation (PEO) process, J. Phys. D. Appl. Phys. 43 (10) (2010), https://doi.org/10.1088/0022-3727/43/10/105203.
[80] F. Jaspard-Mécuson, et al., Tailored aluminium oxide layers by bipolar current adjustment in the Plasma Electrolytic Oxidation (PEO) process, Surf. Coat. Technol. 201 (21) (2007) 8677–8682, https://doi.org/10.1016/j.surfcoat.2006.09.005. SPEC. ISS.
[81] A.B. Rogov, Y. Huang, D. Shore, A. Matthews, A. Yerokhin, Toward rational design of ceramic coatings generated on valve metals by plasma electrolytic oxidation: the role of cathodic polarisation, Ceram. Int. 47 (24) (2021) 34137–34158, https://doi.org/10.1016/j.ceramint.2021.08.324.
[82] I. Shchedrina, A.G. Rakoch, G. Henrion, J. Martin, Non-destructive methods to control the properties of MAO coatings on the surface of 2024 aluminium alloy, Surf. Coat. Technol. 238 (2014) 27–44, https://doi.org/10.1016/j.surfcoat.2013.10.032.
[83] C.B. Wei, X.B. Tian, S.Q. Yang, X.B. Wang, R.K.Y. Fu, P.K. Chu, Anode current effects in plasma electrolytic oxidation, Surf. Coat. Technol. 201 (9-11) (2007) 5021–5024, https://doi.org/10.1016/j.surfcoat.2006.07.103. SPEC. ISS.
[84] X. Nie, E.I. Meletis, J.C. Jiang, A. Leyland, A.L. Yerokhin, A. Matthews, Abrasive wear/corrosion properties and TEM analysis of Al2O3 coatings fabricated using plasma electrolysis, Surf. Coat. Technol. 149 (2002) 245–251.
[85] S. Forero Sotomonte, C. Blanco Pinzon, S.García Vergara, Growth of PEO ceramic coatings on AA 2024-T3 aluminium alloy, in: Journal of Physics: Conference Series, Institute of Physics Publishing, 2016, https://doi.org/10.1088/1742-6596/687/1/012037.
[86] O.P. Terleeva, A.I. Slonova, V.I. Belevantsev, Strength characteristics of 2024 aluminum alloy substrate with plasma electrolytic oxidation coatings, Mater. Res. Express. 5 (9) (2018), https://doi.org/10.1088/2053-1591/aad669.
[87] H. yan Ding, Z. dong Dai, S.C. Skuiry, D. Hui, Corrosion wear behaviors of micro-arc oxidation coating of Al2O3 on 2024Al in different aqueous environments at fretting contact, Tribol. Int. 43 (5–6) (2010) 868–875, https://doi.org/10.1016/j.triboint.2009.12.022.
[88] L. Wen, Y. Wang, Y. Zhou, J.H. Ouyang, L. Guo, D. Jia, Corrosion evaluation of microarc oxidation coatings formed on 2024 aluminium alloy, Corros. Sci. 52 (8) (2010) 2687–2696, https://doi.org/10.1016/j.corsci.2010.04.022.
[89] V.S. Dilimon, S.M.A. Shibli, A review on the application-focused assessment of plasma electrolytic oxidation (PEO) coatings using electrochemical impedance spectroscopy, Adv. Eng. Mater. 25 (12) (2023), https://doi.org/10.1002/adem.202201796.
[90] A. Sobolev, T. Peretz, K. Borodianskiy, Synthesis and growth mechanism of ceramic coatings on an Al-Cu alloy using plasma electrolytic oxidation in molten salt, J. Alloys. Compd. 869 (2021), https://doi.org/10.1016/j.jallcom.2021.159309.
[91] L. Ropyak, T. Shihab, A. Velychkovych, V. Bilinskyi, V. Malinin, M. Romaniv, Optimization of plasma electrolytic oxidation technological parameters of deformed aluminum alloy D16T in flowing electrolyte, Ceramics 6 (1) (2023) 146–167, https://doi.org/10.3390/ceramics6010010.